Coordination of rooting, xylem, and stomatal strategies explains the response of conifer forest stands to multi-year drought in the Southern Sierra Nevada of California

Junyan Ding[1,2], Polly Buotte[3], Roger Bales[4], Bradley Christoffersen[5], Rosie A. Fisher[6,7], Michael Goulden[8], Ryan Knox[1], Lara Kueppers[1,3], Jacquelyn Shuman[6], Chonggang Xu[9], Charles D. Koven[1]

1. Climate and Ecosystem Sciences Division, Lawrence Berkeley National Lab, Berkeley, USA
2. Pacific Northwest National Lab, Richland, WA, USA
3. Energy and Resources Group, University of California, Berkeley, USA
4. Sierra Nevada Research Institute, University of California, Merced, USA
5. Department of Biology, University of Texas, Rio Grande Valley, USA
6. Climate and Global Dynamics Division, National Center for Atmospheric Research, Bold, USA
7. Laboratoire Évolution & Diversité Biologique, CNRS:UMR 5174, Université Paul Sabatier, Toulouse, France
8. Dept. of Earth System Science, University of California, Irvine, USA
9. Earth and Environmental Sciences Division, Los Alamos National Laboratory, Santa Fe, New Mexico, USA

Corresponding author: Junyan Ding (junyan.ding@pnnl.gov)

Key Points:

- We perform a sensitivity analysis using the model FATES-Hydro to explore the co-ordination of leaf, xylem, and root hydraulic traits of pine in Southern Sierra Nevada.
- We find that rooting depth is the major control on water and carbon fluxes, and that deep-rooted pines with risky stomata have the highest GPP but also the highest drought mortality risk.
- Resolving both the plant water sourcing strategies and subsurface processes are critical to represent drought impacts on conifer forests.

Abstract

Extreme droughts are a major determinant of ecosystem disturbance, which impact plant communities and feed back to climate change through changes in plant functioning. However, the complex relationships between above- and belowground plant hydraulic traits, and their role in governing plant responses to drought, are not fully understood. In this study, we use a plant ~~hydraulics~~hydraulic model, FATES-Hydro, to investigate ecosystem responses to the 2012-2015 California drought, in comparison with observations, for a site in the southern Sierra Nevada that experienced widespread tree mortality during this drought.

We conduct a sensitivity analysis to explore how different plant water sourcing and hydraulic strategies lead to differential responses during normal and drought conditions.

The analysis shows that:

1) deep roots that sustain productivity through the dry season are needed for the model to capture observed seasonal cycles of ET and GPP in normal years, and that deep-rooted strategies are nonetheless subject to large reductions in ET and GPP when the deep soil reservoir is depleted during extreme droughts, in agreement with observations.

2) risky stomatal strategies lead to greater productivity during normal years as compared to safer stomatal control, but lead to high risk of xylem embolism during the 2012-2015 drought.

3) for a given stand density, the stomatal and xylem traits have a stronger impact on plant water status than on ecosystem level fluxes.

Our study reveals the importance of resolving plant water sourcing strategies in order to represent drought impacts on plants, and consequent feedbacks, in models.

1. Introduction

Understanding plant water use strategies and the resulting ecohydrologic processes in forests is critical for predicting surface water and energy exchange, carbon dynamics and vegetation dynamics of water-constrained ecosystems in a changing climate. Mediterranean-type climates, as in California, are characterized by dry and hot summers and cool, wet winters, resulting in asynchronous supplies of energy and water. In addition to these climatic stresses, plants in California are further subject to high inter-annual variability in precipitation, and periodic severe drought events, such as the recent 2012 – 2015 drought, which led to widespread tree mortality (Fettig et al. 2019). Together, these two climatic constraints bring a unique challenge to the success of forests in California, which are likely to be exacerbated in a warming climate.

On evolutionary timescales, natural selection has led to a wide array of strategies and functional traits that allow plants to both grow and survive under a range of environment conditions (Grime 1977,1979; Coley et al. 1985; Westoby et al. 2002; Craine 2002; Reich et al. 2003). Given the centrality of water sourcing on plant physiology, plant hydraulic traits play an important role in water-constrained ecosystems. Once absorbed by fine roots, water flows through the vascular system via coarse roots, stems, branches, to leaves where it evaporates through stomata. The rate of water flow through stems, and thus the supply to leaves, is determined by the hydraulic conductivity along this pathway. If the water potential of xylem tissue becomes too low, cavitation can occur and cause a loss of conductivity. Because this cavitation can damage the xylem network, trees have developed different strategies to mitigate this effect, all of which come at some cost. These strategies include 1) early stomatal closure or leaf deciduousness to reduce the flow of water, at the cost of reduced carbon intake; 2) building cavitation-resistant xylem, at the cost of increased hydraulic resistance; and 3) growing deep roots to access more moisture, at the cost of higher carbon investment. In this study, we focus on the potential hydraulic strategies that trees in Californian ecosystems use, with a particular emphasis on how the co-ordination of hydraulic functional traits at the leaf, stem, and root levels is critical to carbon assimilation, transpiration, and consequently, the productivity and the response of trees to drought (Matheny, Mirfenderesgi, and Bohrer 2017; Matheny et al. 2017; Mursinna et al. 2018a).

88   The traits that regulate stomatal conductivity are the most important hydraulic traits of
89   leaves and the primary ones through which photosynthesis and transpiration are coupled.
90   Stomatal behavior falls along a gradient between two extremes: stomata may close early during
91   water stress to avoid the risk of hydraulic failure, or remain open to maximize carbon uptake
92   while exposing xylem to a higher risk of embolism (Martínez-Vilalta, Sala, and Piñol 2004;
93   McDowell et al., 2008; Skelton, West, & Dawson, 2015, Matheny et al. 2017). The sensitivity of
94   stomata to water stress determines where the stomata operate along the safety-risky gradient, and
95   thus the degree that carbon intake is traded for preventing the cavitation of xylem. Where the
96   best stomatal strategy sits along the safety-risky gradient would depend on the physical
97   environment.

98   The maximum hydraulic conductivity and the vulnerability to cavitation are the two key
99   xylem hydraulic traits. Differences in the anatomy and morphology of the conductive xylem cell
100   structure and anatomy (Hacke et al. 2017) lead to differences in maximum conductivity and the
101   water potential at which cavitation starts to occur (Pockman & Sperry, 2000; Sperry 2003).
102   Within the conifers, there are at least three mechanisms that lead to a tradeoff between xylem
103   safety and efficiency. First is the morphology of the xylem conduit. It is widely acknowledged
104   that narrow (or short) tracheid are safer than wider (or longer) tracheid but have lower
105   conductance per sap area (Choat and Pittermann 2009). Second are the intervessel pit
106   membranes. Thicker and less porous membranes prevent the spread of air but increase the
107   hydraulic resistance of xylem (e.g. Li et al., 2016; Pratt & Jacobsen 2017). The third mechanism
108   comes from the division of limited space (Pratt and Jacobsen 2017). With the same cross
109   sectional area of conduits, vessels with a thicker cell wall provide stronger mechanical support,
110   so that the conduits are less likely to collapse when xylem water potential becomes more
111   negative, however this reduces the area that can be used for conduits transporting water. While
112   these physiological constraints require that the tradeoff does exist to some extent, in many
113   studies, this tradeoff appears to be weak, and there are certainly species that have both safe and
114   efficient xylem. Further, there are many other plant traits that can affect the safety, such as wood
115   density (Pratt and Jacobsen 2017), pit anatomy (Sperry & Hacke 2004, Lens et al. 2011), and
116   biochemistry (Gortan et al. 2011). These traits can have large variation among thedifferent
117   plant types. The tradeoff will be weakened when grouping plants inat a coarse scale, e.g., by
118   biomass, families and/or across a range of geological and climatic region. But when focusing on

119 certain species in a particular region, the tradeoff becomes stronger, as demonstrated by many

120 local studies (e.g Barnard et al. 2011, Corcuera et al. 2011, Baker et al. 2019). For example,

121 Kilgore et al. (2021) shows that there is a clear safety-efficiency tradeoff ~~of the~~across   pine

122 trees in a specific location in the western US. Thus, while we acknowledge that there are many

123 exceptions to the xylem safety-efficiency tradeoff, it is a useful framework for examining plant

124 strategies for dealing with drought.

125   The traits that govern the hydraulic function of plant root systems are also critically

126 important, but the least understood ~~and,~~   studied, and quantified. These traits include the

127 rooting depth, the root to shoot ratio, the vertical and lateral distribution of roots, and the fine

128 root density and ~~diameters~~diameter   , all of which are related to water uptake (Canadell et al.,

129 2007, Allen 2009, Reichstein et al., 2014, Wullschleger et al. 2014). In general, species with

130 deeper roots can access water at greater depths, that is unavailable to more shallowly rooted

131 species (Jackson et al., 1996; Canadell et al., 1996). The vertical root distribution can affect the

132 water uptake and thus the evapotranspiration (ET) pattern during the dry-down period (Teuling,

133 Uijlenhoet, and Troch 2006). This in turn affects the seasonal distribution of water over the soil

134 depth, and thereby the resilience of plants to seasonal droughts (Yu, Zhuang, and Nakayamma

135 2007). The vertical root distribution is also a means of belowground niche differentiation (Ivanov

136 et al. 2012; Kulmatiski and Beard 2013), whereas the extent of the lateral root distribution

137 dictates the competition ~~of~~for   water (Agee et al. 2021). Whether a plant can benefit from

138 having deep roots is related to the plant's leaf and xylem hydraulic traits (e.g. Johnson et al.

139 2018, Mackay et al. 2020), thus requiring coordination of rooting and hydraulic traits.

140   Given the strength of the Mediterranean-type climate of California, the coordination of

141 rooting and hydraulic strategies will play a critical role for ~~the~~   forest dynamics. However, the

142 interplay of rooting and hydraulic strategies and their impact on ecosystem processes haven't

143 been well understood. In this study, we address this question at the Soaproot site (CZ2) of the

144 southern Sierra Nevada of California as the study area. The CZ2 site was strongly affected by the

145 2012-2015 drought, with extremely high tree mortality rates (~90% of the pine died) (Fettig et al.

146 2019). While the 2012 - 2015 drought was widespread across California, the highest rates of tree

147 mortality occurred in the southern Sierra Nevada, centered around an elevation similar to this site

148 (1160 m to 2015 m, Asner et al. 2016, Goulden and Bales 2019). This mid-elevation region is

149 also characterized by the highest forest productivity along an elevation gradient from foothill

150 woodlands to subalpine forest (Kelly and Goulden 2016). This leads us to ask whether strategies

151 associated with high productivity have exposed trees to high mortality risk under prolonged

152 drought.

153   Specifically, here we use the Functionally Assembled Terrestrial Ecosystem Simulator, in

154 a configuration that includes plant hydraulics (FATES-Hydro), to explore the tradeoffs

155 associated with differing hydraulic strategies, and in particular their implications for plant

156 productivity and risk of drought-induced mortality. We conduct a sensitivity analysis, using

157 FATES-Hydro in comparison with observations from the CZ2 eddy covariance site, to

158 investigate how stomatal, xylem and rooting strategies affect the ecosystem and physiologic

159 processes of the forest, and whether that may explain the high rates of both productivity and

160 drought-associated mortality of conifers at CZ2. We note that this is not an exhaustive

161 model parameter sensitivity study. The main purpose is to use a sensitivity analysis to

162 explore scientific questions around hydraulic trait tradeoffs.

163 **2. Methods**

164 2.1 Study site

165   The Soaproot site is a 543-ha headwater catchment at 1100m elevation (37°2.4' N,

166 119°15.42' W), which is at the lower boundary of the rain–snow transition line with warm, dry

167 summers and cool, wet winters (Geen et al. 2018). The mean annual temperature is about 13.8°C

168 (Goulden et al., 2012). Under normal conditions, the annual precipitation is about 1300 mm, but

169 during a dry year, the precipitation can drop to 300-600mm. (Bales et al. 2018). The site is a

170 ponderosa pine (*Pinus ponderosa*) dominated conifer ecosystem exhibiting high productivity

171 (Kelly and Goulden (2016) reported 2.1 tC/ha/year average annual gross stem wood production

172 averaged). Other species include California black oak (*Quercus kelloggii* Newberry), and incense

173 cedar (*Calocedrus decurrens*).

174   Soils at the Soaproot site are mainly of the Holland (fine-loamy, mesic Ultic Haploxeralfs)

175 and Chaix (coarse-loamy, mesic Typic Dystroxerepts) series, which are representative of soils

176 across a similar elevation band of the western Sierra Nevada (Mooney and Zavaleta 2003). Soils

177 of the Holland series have sandy loam surface texture and underlying Bt horizons with sandy

178 clay loam textures, while soils of the Chaix series have sandy loam textures throughout the

179 profile. The regolith depth is estimated to be 15m (Holbrook et al., 2014). The total porosity over

180 the whole regolith depth of the site is estimated to be 1620 mm and the total available storage

181 porosity (plant accessible water storage capacity), which is the difference in volumetric water

182 content between field capacity and permanent wilting point (~ -6Mpa) to be 1400 mm (Klos et

183 al. 2017). The available water storage capacity is approximately 0.20 cm^3 cm^{-3} in the upper

184 regolith (0–5 m depth) which decreases to 0.05 cm^3 cm^{-3} or less in the lower regolith (below 5

185 m depth) (Holbrook et al., 2014).

186   An eddy-covariance flux tower was installed at this site in September 2010. The elevation

187 of the tower is 1160 m above sea level. Instruments on the flux tower track changes in carbon

188 dioxide, water vapor, air temperature, relative humidity, and other atmospheric properties. We

189 compare the simulated gross primary productivity (GPP) and latent heat flux with the flux tower

190 measurements over the period from 2011 to 2015 (Goulden and Bales 2019). We computed the

191 Root Mean Square Error (RMSE) of the hourly mean diurnal cycle of each month. This allows

192 us to examine the capacity of FATES-Hydro to predict the carbon and water fluxes. The

193 transpiration ofat   the site contributed to the majority of the ET as indicated by the

194 measurements from an adjacent catchment, as well as the fact that the site is fully vegetated with

195 an annual LAI around 3 to 4.

196

197 2.2 FATES-Hydro model and parameterization

198 2.2.1 The FATES-Hydro model

199   FATES is a cohort-based, size- and age-structured dynamic vegetation model, where long-

200 term plant growth and mortality rates and plant competition emerge as a consequence of

201 physiological processes. In the model, multiple cohorts grow on the same land unit, share the soil

202 water, and interact with each other through light competition. FATES is coupled within both the

203 CLM5 (Lawrence et al., 2019) and the ELM (Golaz et al., 2020) land surface models (LSMs). In

204 this study, FATES is coupled with the CLM5. FATES-Hydro is a recent development of the

205 FATES model (Fisher et al., 2015; Koven et al., 2020), in which a plant hydro-dynamic module,

206 originally developed by Christoffersen et al. (2016), wasis   coupled to the existing

207 photosynthesis and soil hydraulic modules. FATES-Hydro is described in more detail by Xu et

208 al., (in review, https://doi.org/10.5194/egusphere-2023-278) and its supplementary material.

209   Conceptually, plant hydraulic ~~modules~~models can be broadly grouped into ~~to~~ two

210 types. The first group represents the plant hydraulic system as analogous to an electrical circuit

211 (e.g. Mackay et al. 2011, Huang et al. 2017, Eller et al. 2018, Kennedy et al. 2019). The total

212 resistance of the plant is calculated from the resistance of each compartment using Ohm's law.

213 There is no storage of water in the plants and the transpiration from plants at any given time step

214 is considered to ~~be completed~~come directly from soil storage. The second group represents

215 plant hydraulics by a series of connected porous media, corresponding to each plant

216 compartment (e.g. Bohrer et al. 2005~~),~~, Janott et al. 2011, Xu et al., 2016, Christoffersen et al.,

217 2016). The porous media model takes into account the water storage in the plant. The flow

218 between two adjacent compartments is driven by the difference in the water potential, mediated

219 by the hydraulic conductivity. FATES-Hydro falls in the second group. The various models in

220 the second group differ in the exact formulas used to describe the pressure-volume and pressure-

221 conductivity relations, as well as different numbers and arrangement of nodes within the soil-

222 plant-atmosphere system.

223   In FATES-Hydro, for each plant cohort, the hydraulic module tracks water flow along a

224 soil–plant–atmosphere continuum of a representative individual tree based on hydraulic laws,

225 and updates the water content and potential of leaves, stem, and roots with a 30 minute model

226 time step. Water flow from each soil layer within the root zone into the plant root system is

227 calculated as a function of the hydraulic conductivity as determined by root biomass and root

228 traits such as specific root length, and the difference in water potential between the absorbing

229 roots and the rhizosphere. The vertical root distribution is based on Zeng's (2001) two parameter

230 power law function which takes into account the regolith depth:

$$Y_i = \frac{0.5(e^{-r_a z_{li}} + e^{-r_b z_{li}}) - 0.5(e^{-r_a z_{ui}} + e^{-r_b z_{ui}})}{1 - 0.5(e^{-r_a z} + e^{-r_b z})} \qquad Y_i = \frac{0.5(e^{-r_a z_{li}} + e^{-r_b z_{li}}) - 0.5(e^{-r_a z_{ui}} + e^{-r_b z_{ui}})}{1 - 0.5(e^{-r_a z} + e^{-r_b z})},$$

232   (Eq 1)

233 where Y_i is the fraction of fine or coarse roots in the ith soil layer, r_a and r_b are the two

234 parameters that determine the vertical root distribution, Z_{li} is the depth of the lower boundary of

235   the ith soil layer, and Z_{ui} is the depth of the upper boundary of the ith soil layer, and Z is the total

236   regolith depth. The vertical root distribution affects water uptake by the hydrodynamic model by

237   distributing the total amount of root, and thus root resistance, through the soils.

238   The total transpiration of a tree is the product of total leaf area (LA) and the transpiration

239   rate per unit leaf area (J). ~~In this version of FATES-Hydro, we adopt the model developed by~~

240   ~~Vesala et al. (2017)~~In this version of FATES-Hydro, we adopt the model developed by Vesala et

241   al. (2017) to take into account the effect of leaf water potential on the within-leaf relative

242   humidity and transpiration rate:

243

$$E = LA \cdot J \tag{Eq 2a}$$

$$J = \rho_{atm} \frac{(q_l - q_s)}{1/g_s + r_b} \tag{Eq 2b}$$

$$q_l = \exp(\frac{k_{LWP} \cdot LWP \cdot V_{H2O}}{R \cdot T}) \cdot q_{sat} \tag{Eq 2c}$$

244

$$E = LA \cdot J \tag{Eq 2a}$$

$$J = \rho_{atm} \frac{(q_l - q_s)}{1/g_s + r_b} \tag{Eq 2b}$$

$$q_l = \exp(\frac{w \cdot LWP \cdot V_{H2O}}{R \cdot T}) \cdot q_{sat} \tag{Eq 2c}$$

245   where E is the total transpiration of a tree, LA is the total leaf area (m^2), J is the transpiration per

246   unit leaf area (kg s^{-1} m^{-2}), ~~ρ_{atm}~~ ρ_{atm} is the density of atmospheric air (kg m^{-3}), ~~q_l~~ q_l is the within-

247   leaf specific humidity(kg~~/~~ kg^{-1}), ~~q_s~~ q_s is the atmosphere specific humidity (kg~~/~~ kg^{-1}), ~~g_s~~ g_s

248   is the stomatal conductance per leaf area, ~~r_b~~ r_b is the leaf boundary layer resistance(s m^{-1}), k_{LWP}

249   w is a scaling coefficient (unitless), which can vary between 1 and 7, and here we use a value of

250   3; LWP is the leaf water potential (Mpa), ~~V_{H2O}~~ V_{H2O} is the molar volume of water (18 × 10^{-6} m^3

251   mol^{-1}), R is the universal gas constant, and T is the leaf temperature (K).

252   The sap flow from absorbing roots to the canopy through each compartment of the tree

253   along the flow path- way (absorbing roots, transport roots, stem, and leaf) is computed

according to Darcy's law in terms of the plant sapwood water conductance, the water potential gradient:

$$Q_i = -K_i[\rho_w g(z_i - z_{i+1}) + (\Psi_i - \Psi_{i+1})]$$

(Eq 3)

where ρ_w is the density of water; z_i is the height of the compartment(m); z_{i+1} is the height of the next compartment down the flow path (m); Ψ_i is the water potential of the compartment(Mpa); Ψ_{i+1} is the water potential of the next compartment down the flow path(Mpa); and K_i is the hydraulic conductivity of the compartment (kg Mpa^{-1} m^{-1} s^{-1}). The hydraulic conductivity of the compartments is by the water potential and maximum hydraulic conductivity of the compartment through the pressure-volume (P-V) curve and the vulnerability curve (Manzoni et al. 2013, Christoffersen et al. 2016).

The plant hydrodynamic representation and numerical solver scheme within FATES-HYDRO follows Christoffersen et al. (2016). We made a few modifications to accommodate the multiple soil layers and to improve the numerical stability. First, to accommodate the multiple soil layers, we have sequentially solved the Richards' equation for each individual soil layer, with each layer-specific solution proportional to each layer's contribution to the total root-soil conductance. Second, to improve the numerical stability, we have an option to linearly extrapolate the PV curve beyond the residual and saturated tissue water content to avoid the rare cases of overshooting in the numerical scheme under very dry or wet conditions. Third, Christoffersen et al. (2016) use three phases to describe the PV curves: 1) dehydration phases representing capillary water (sapwood only), 2) elastic cell drainage (positive turgor), and 3) continued drainage after cells have lost turgor. Due to the possible discontinuity of the curve between these three phases, it leads to the potential for numerical instability. To resolve this instability, FATES-HYDRO added the Van Genuchten model (Van Genuchten 1980, July and Horton 2004) and the Campbell model (Campbell 1974) as alternatives to describe the PV curves.

280   In this study, we use the Van Genuchten model because of two advantages: 1) it is simple,

281 with only three parameters needed for both curves, and 2) it is mechanistically based, with both

282 the P-V curve and vulnerability curve derived from a pipe model, and thus connected through

283 three shared parameters:

284

$$\Psi = \frac{1}{-\alpha} \cdot \left(\frac{1}{Se^{1/m}} - 1 \right)^{1/n} \tag{Eq 4a}$$

$$FMC = \left(1 - \left(\frac{(-\alpha \cdot \Psi)^n}{1 + (-\alpha \cdot \Psi)^n} \right)^m \right)^2 \tag{Eq 4b}$$

285

$$\Psi = \frac{1}{-\alpha} \cdot \left(\frac{1}{Se^{1/m}} - 1 \right)^{1/n} \tag{Eq 4a}$$

$$FMC = \left(1 - \left(\frac{(-\alpha \cdot \Psi)^n}{1 + (-\alpha \cdot \Psi)^n} \right)^m \right)^2 \tag{Eq 4b}$$

286 where Ψ is the water potential of the media (xylem in this case) (Mpa); FMC is the

287 fraction of xylem conductivity, K/K_{max}, (unitless); α is a scaling parameter for air entry point

288 (Mpa^{-1}), Se is the dimensionless standardized relative water content as $Se = (\theta - \theta_r)/(\theta_{sat} - \theta_r)$

289 $Se = (\theta - \theta_r)/(\theta_{sat} - \theta_r)$ with θ, θ_r, θ_{sat} are volumetric water content (m^3 m^{-3}), residual

290 volumetric water content, and saturated volumetric water content correspondingly; and m and n

291 are dimensionless (xylem conduits) size distribution parameters. The model assumes that xylem

292 conductance can be restored as xylem water content increases due to increased water availability

293 after a dry period without any hysteresis in the FMC curve.

294

295   The stomatal conductance is modelled in the form of the Ball-Berry conductance model

296 (Ball et al. 1987, Oleson et al. 2013, Fisher et al. 2015):

$$g_s = b_{slp}\frac{A_n}{c_s / P_{atm}}\frac{e_s}{e_i} + b_{opt}\beta_t \qquad g_s = b_{slp}\frac{A_n}{c_s / P_{atm}}\frac{e_s}{e_i} + b_{opt}\beta_t ,$$

(Eq 5)

where b_{slp} and b_{opt} are parameters that represent the slope and intercept in the Ball-Berry model, correspondingly. These terms are plant strategy dependent and can vary widely with plant functional types (Medlyn et al. 2011). The parameter b_{opt} is also scaled by the water stress index β_t. A_n is the net carbon assimilation rate (µmol CO2 m^{-2} s^{-1}) based on Farquhar's (1980) formula. This term is also constrained by water stress index β_t in the way that the $V_{cmax,25}$ is scaled by β_t as $V_{cmax,25}\beta_t$ (Fisher et al. 2018). c_s is the CO$_2$ partial pressure at the leaf surface (Pa), e_s is the vapor pressure at the leaf surface (Pa), e_i is the saturation vapor pressure (Pa) inside the leaf at a given vegetation temperature when $A_n = 0$.

The water stress index β_t, a proxy for stomatal closure in response to desiccation, is determined by the leaf water potential adopted from the FMC$_{gs}$ term from Christoffersen et al. (2016):

$$\beta_t = \left[1 + \left(\frac{\Psi_l}{P50_{gs}}\right)^{ags}\right]^{-1} \qquad \beta_t = \left[1 + \left(\frac{\Psi_l}{P50_{gs}}\right)^{ags}\right]^{-1}$$

(Eq 6)

where Ψ_l is the leaf water potential (MPa), $P50_{gs}$ is the leaf water potential of 50% stomatal closure, and ags governs the steepness of the function. For a given value of ags, the $P50_{gs}$ controls the degree of the risk of xylem embolism (Christoffersen et al. 2016, Powell et al. 2017).(Christoffersen et al. 2016, Powell et al. 2017). A more negative $P50_{gs}$ means that, during leaf dry down from full turgor, the stomatal aperture stays open and thus allows the transpiration rate to remain high and xylem to dry out, which thus can maintain high photosynthetic rates, at the risk of exposing xylem to embolism and thus plant mortality. Conversely, a plant with a less negative $P50_{gs}$ will close its stomata quickly during leaf dry down, thus limiting transpiration

320 and the risk of xylem embolism and mortality associated with it, at the cost of reduced
321 photosynthesis.

322

323 2.2.2 Sensitivity analysis and Parameterization

324   The goal of this analysis is to better understand how coordinated aboveground and
325 belowground hydraulic traits determine plant physiological dynamics and the interplay between
326 ecosystem fluxes and tissue moisture during the extreme 2012-2015 drought at the Soaproot site.
327 We thus conduct a global sensitivity analysis on selected hydraulic parameters to explore the
328 linkages of aboveground and belowground hydraulic strategies. We use a full-factorial design for
329 the parameter sensitivity analysis in order to best investigate the relationships between
330 parameters. Because this design requires a relatively small set of parameters or groups of
331 parameters to vary, we chose parameters that represent the major axes of relatively well-
332 understood stomatal, xylem and rooting mechanisms/strategies that control the hydraulic
333 functioning of trees. We set the values of these parameters within the realistic (allowable
334 biological) range based on online database, and literatures where the species and physical
335 environment are as close to our system as possible. We list other major parameters and their
336 estimates that are not varied in the sensitivity analysis (table 2). We acknowledge that the biggest
337 disadvantage of this study is the lack of sufficient field data to constrain the model. This is a
338 result of using a natural drought as an experiment of opportunity, which because it was not
339 anticipated, did not allow for as coordinated planning as would be the case in an experimentally-
340 manipulated drought. The trees at that site had all died by the time we started this study.

341   The parameters that we vary here are 1) the pair of r_a and r_b, which control vertical root
342 distribution as deep vs shallow roots, 2) two sets of xylem parameters (P_{50x}, K_{max}, m, n, and α)
343 that jointly represent two distinct xylem strategies: efficient/unsafe and inefficient/safe xylem
344 within the range observed for temperate conifer trees, and 3) the stomatal parameter $P50_{gs}$, which
345 represents the stomatal strategy along a risky to safe gradient (Table 1). The ranges of root
346 parameters are chosen so that the effective rooting depth, above which 95% of root biomass
347 stays, varies from 1m to 8m which is the possible range at the Soaproot site, as indicated by
348 current knowledge of the subsurface structure (see Klos et al., 2017). Note, here we refer to a
349 higher proportion of roots in deep subsurface layers as 'deep rooting' (e.g effective rooting depth

350   = 8m; r_a=0.1,r_b=0.1) as compared to 'shallow rooting' (e.g effective rooting depth = 2; r_a=1,r_b=5)

351   which represents a larger proportion of fine roots in upper layers (Figure 1a).

352   The safety-efficiency tradeoff of xylem has been widely discussed in the literature (e.g.

353   Gleason et al. 2016; Hacke et al. 2006, 2017; Martnez-Vilalta, Sala, and Piol 2004). Given that

354   we don't have any measurements that can be used to ~~a~~ generate vulnerability curve at our study

355   site, we consult the literature (Domec et al. 2004, Barnard et al. 2011, Corcuera et al. 2011,

356   Anderegg and Hillerislambers 2016 , Baker et al. 2019, Kilgore et al. 2021) for observed curves

357   from sites that ~~have~~ are as similar both in climate (e.g mean annual precipitation and

358   temperature) and in the set of conifer species (P. Ponderosa) to our study site as possible ~~and~~

359   ~~the~~ , as well as values of xylem traits (K_{max} and $P50_x$) of Ponderosa pine in temperate

360   regions of the TRY database (Kattge et al. 2020) to determine the two hypothetical vulnerability

361   curves representing the safe/inefficient and unsafe/efficient xylem strategies. We set the

362   parameters of the van Genuchten model to represent these two sets of P-V and vulnerability

363   curves as ~~showing~~ shown in Fig1b and 1c. It is worth noting that with the same K_{max} and $P50$,

364   the exact shape of the vulnerability can ~~be different depends~~ differ depending on the

365   formula used and parameter values. However, this should not be an issue in our study because

366   the vulnerability curve is mainly constrained by P50 and Kmax. Second, given that there is a

367   large range of variation ~~of~~ in the ~~observed/~~ measured values, the effect caused by the exact

368   shape of the curves is minor. Third, since the objective of our study is not to accurately predict

369   mortality, but rather to examine the effect of different combination of stoma, xylem, and root

370   strategies, even if the shape of our vulnerability curve is not the most accurate, as long as the

371   curve captures the overall pattern of the pressure-conductivity relation, it will not affect the

372   relative outcome of this study.

373   We follow the theory of Skelton et al. (2015) to define safe vs. efficient stomatal strategy.

374   In FATES-Hydro, there are two key stomatal parameters: $P50_{gs}$ and a_{gs}. Here, we only vary

375    $P50_{gs}$ while keeping a_{gs} as a constant because the objective here is to choose the parameters that

376   are relatively well understood and to catch the safe vs. risky strategies as described by Skelton et

377   al., rather than to exhaust the parameter space ~~throughout~~ within the model. In essence, the

378   different combinations of $P50_{gs}$ and the shape parameter (a_{gs}) can generate similar stomatal

379   response curves. For example, a small negative $P50_{gs}$ with small a_{gs} would result in a flat

380 stomatal response curve, which is similar to a large negative $P50_{gs}$ combined with a large a_{gs}.

381 Further, $P50_{gs}$ is well understood and has more observed data, while a_{gs} is less studied and barely

382 has any observed data. With a given a_{gs}, the variance of $P50_{gs}$ ~~along~~ for a given Pxylem

383 value, ~~vulnerability curve~~ controls the degree of embolism risk, from a 'risky' strategy, where

384 $P50_{gs}$ is equals to ~~a~~or lower than P_{xylem}, to a 'conservative' strategy, where $P50_{gs}$ ~~equals a~~ is

385 higher than P_{xylem}. The $P_{xylem}s$ in Skelton et al.'s (2015) are for Fynbos species, therefore are not

386 appropriate for our study because our species are pine trees, a woody plant. Trees have woody

387 tissue which contribute to strengthen the conduits and make them less easy to collapse when

388 embolized, hence allow their stomata to be riskier than herbaceous plants. From the observed

389 $P50_{gs}$ and xylem traits of closely related pine species in the TRY database (Kattge et al. 2020)

390 and elsewhere in the literature (Bartlett et al. 2016), as well as the observed soil water potential

391 at the study site, we choose to vary $P50_{gs}$ between $P50_{xylem}$ and $P20_{xylem}$, (correspondingly the

392 point at which xylem have lost 50% and 20% of their maximum conductivity).

393   The emergent behavior of FATES or any model with dynamic ecosystem structure can

394 make analysis of physiological rate variation difficult, as the stand structure will respond and

395 thus also vary when parameters are changed. Here, we wanted to first understand the direct trait

396 control in the absence of structural differences. To overcome ~~this~~ complication of the dynamic

397 structure, we use a reduced complexity configuration for running the model which we refer to as

398 'static stand structure' mode. To investigate dynamic competitive effects when growth and

399 mortality will be the next step. In this mode, the stand structure is initialized from observed

400 forest census data, and subsequently is fixed, i.e. the model does not permit plant growth or death

401 to change the vegetation structure. This allows the direct assessment of hydraulic and

402 physiological parameter variation in the model without the consequent feedback loops associated

403 with varying ecosystem structure. The stand structure is initialized with census data from the

404 CZ2 site (Table S1~~).~~) and thus includes multiple cohorts of different sized trees. Because this

405 type of model configuration ignores prognostic plant mortality, in the interest of being able to

406 compare across simulations where mortality rates might otherwise be very high, we use the loss

407 of xylem conductivity as a measure of mortality risk of conifer trees at CZ2, which has widely

408 been used as an indicator of drought mortality of forest (e.g. Hammond et al., 2019).

409   To force the model with an atmospheric upper boundary, we use the Multivariate Adaptive

410   Constructed Analogs (MACA) climate data (Abatzoglou and Brown 2012) from 2008 – 2015 of

411   a 4km x 4km grid covers the study area. The daily average MACA data are disaggregated to 3-

412   hourly climate data (see Appendix S2 in Buotte et al. 2018 for detail)~~. To assess the credibility~~

413   ~~of model predictions, we compare the model to observations of gross primary productivity (GPP)~~

414   ~~and ET, both as inferred from eddy covariance (Goulden and Bales 2019). Here, we use the~~

415   ~~Latent Heat Flux (LH) is used as a proxy of ET.~~ . We set the initial soil water content to be

416   75% of saturated water content, close to field capacity. We believe this is a realistic value

417   because the model is initialized in January, when the study area has high precipitation and trees

418   are all in a dormant status, and in a year when there is not drought. We also tried to initialize the

419   soil with higher water content (e.g. saturation), but did not find any differences, as the extra

420   water drained quickly in the winter when transpiration is low.

421   **3. Results**

422   3.1 ~~Impact on~~Sensitivity of GPP and ET to parameter perturbations

423   The parameter sensitivity analysis shows that in a monthly-mean flux comparison, the

424   simulations with deep roots give a better match to the overall observed pattern of GPP and ET

425   (Fig. 2). The simulated transpiration contributes to 90% of the ET in general. The deep-rooted

426   cases better capture the seasonality (e.g. the peak time) and the declining trend of observed GPP

427   from 2011 to 2015. The deep-rooted cases also match fairly well the observed ET. The simulated

428   GPP of shallow-rooted cases are higher than observed values during wet seasons (Dec. to Mar.),

429   but much lower than the observed values during dry season of the pre-drought period. The

430   simulated ET of shallow-rooted cases are overall lower than the observed values. To quantify

431   this assessment, we computed Root Mean Square Error (RMSE) from the hourly mean GPP and

432   ET of each month each year of all the 40 cases (Fig. S2). We choose RMSE as it is a common

433   and compact metric of assessing model performance, though we note that other metrics could in

434   principle be used, each of which has different advantages and disadvantages (e.g. Collier et al.,

435   2018). The RMSE of GPP and ET decreases with both effective rooting depth and P50gs for

436   both xylem strategies (Fig. 3). The P50gs has less impact on the RMSE of GPP ~~of~~for the case

437   with safe xylem than on that of the case with efficient xylem. In terms of GPP, the effective

438   rooting depth of 6.5m gives the best fit, as indicated by the darkest color (RMSE of GPP =

439   1.12gC/m^2/s, RMSE of ET = 250 W/m^2), ~~suggesting~~underscoring   the importance of deep roots

440   in maintaining transpiration and photosynthesis during the dry season, as well as the role of deep

441   roots in increasing the relative decline in these fluxes during the drought.

442   Among the parameters we varied in the sensitivity analysis, the vertical root distribution

443   has the largest impact on GPP and ET at CZ2. Figures 2a-2b show the monthly mean GPP and

444   ET of the end members of the sensitivity analysis (see Fig. S1 for the complete set of outcomes).

445   We acknowledge that the variation in rooting depth across the ensemble is large, but point out

446   that so is uncertainty in plant rooting depth, and moreover that the uncertainty in rooting depth is

447   less well-quantified than other plant traits such as P50, such that this wide variation reflects a

448   real and deep uncertainty in plant rooting profiles. Deep roots result in substantially higher GPP

449   and transpiration during normal years (2011 and 2012). During long-term droughts, when deep

450   soil moisture is depleted, the relative advantage of deep roots over shallow roots is reduced.

451   Shallow roots result in substantially lower GPP and transpiration during the dry season (Aug. to

452   Oct.), with seasonal maximum occurring earlier, in May, as compared to July with the deep-

453   rooted cases. The shallow-rooted cases also have much lower GPP and ET during the dry

454   seasons of the pre-drought period. During the late stage of drought (2014 and 2015), the GPP and

455   ET of the different cases become more similar between the shallow- and deep-rooted cases.

456   The second set of parameters in importance to rooting depth for controlling carbon and

457   water fluxes is the stomatal strategy. The simulations with a more risky strategy (P50$_{gs}$=P50$_x$)

458   gives higher GPP and ET than the simulations with a safer strategy (P50$_{gs}$=P20$_x$) during pre-

459   drought periods and the early stage of the drought (2011 to 2013), but slightly lower GPP and ET

460   at the late stage of the drought (2014 and 2015) for the deep-rooted cases. However, risky

461   stomata gives slightly higher GPP and ET at all times for shallow-rooted cases. The xylem

462   strategy has the smallest effect on GPP and ET of the parameters we varied (e.g~~.~~., RMSEs of ET

463   are both around 260 W/~~m2~~m^2 for safe and efficient xylem, respectively, with P50gs = P20x and

464   8m effective rooting depth). In deep-rooted cases, the safe xylem and efficient xylem strategy

465   result in almost the same GPP and ET, which can be seen via the ~~widespread~~wides   overlap

466   between the dashed and solid lines in figure 1. In shallow-rooted cases, with safe stomata, safe

467   xylem generates slightly higher GPP and ET than efficient xylem. In addition, ~~how strong~~   the

468   strength of effects of stomatal and xylem strategy also depend on the rooting depth. The deeper

469   the effective rooting depth, the less significant the impacts of stomatal strategy (Fig. S1).

470

471   3.2 Impact onSensitivity of   plant water status to parameter perturbations

472   We examine the impact of vertical root distributions, stomatal and xylem strategies on the

473   seasonal variation of three plant physiologic variables that serve as indices of plant water stress

474   (fig. 4): the fraction loss of xylem conductivity of stem (SFL), leaf water potential (LWP), and

475   an overall absorbing rootsroot   water potential (AWP). In the model, absorbing roots in

476   different soil layers have different water potentials, associated with the soil water potential of

477   that layer. We calculate a cohort-level effective AWP as the root-fraction--   weighted average

478   of water potential in absorbing root across all soil layers. In this way, the AWP represents the

479   overall rhizosphere soil moisture condition that is sensed by the tree. These physiological

480   variables are tracked for each cohort. For any given case, the differences in these variables

481   among differently-sized cohorts are negligible (Fig. S3). Therefore, we present the outcome of

482   theall   cohort class s   with a diameter at breast height (DBH) between 50 – 60cm, the size

483   class that is most abundant at CZ2.

484   Stomatal and rooting strategies together control the loss of xylem conductivity during the

485   dry season of the pre-drought period and the whole period of the long-term drought (Fig 4a). In

486   all cases, the xylem conductivity reaches a maximum during the wet season (Dec. to Jan.), starts

487   to decline during the growing season (Apr. to Jun.), then reaches its minimum in the dry season.

488   With the same stomatal strategy, deep roots lead to less-extreme loss of xylem conductivity than

489   shallow roots. A deep rooting strategy is also able to maintain very little loss of   xylem

490   conductivity with very little seasonal loss during the pre-drought period, but as deep soil

491   moisture is depleted, this effect is reduced. With a shallow rooting profile, the xylem

492   conductivity starts to decline earlier and the minimum is much lower than that of a deep rooting

493   profile. For example, with risky stomata, the minimum fraction of xylem conductivity of deep-

494   rooted cases atin   2012 is 0.4, but is lower than 0.2 with shallow roots. Unlike deep-rooted

495   cases, in shallow-rooted cases, the seasonal variation of the loss of xylem conductivity does not

496   differ too much during pre-drought and drought periods. During the very late stage of the

497 drought, deep-rooted cases have a lower fraction of xylem conductivity than shallow-rooted
498 cases (e.g., in Jan. 2015).

499 In general, risky stomata ~~cause~~allow a greater loss of xylem conductivity (K/Kmax) than
500 safe stomata, but the extent depends on the vertical root distribution. The effect of the stomatal
501 strategy is more obvious in shallow-rooted cases. Risky stomata combined with shallow roots
502 ~~results~~result in increasing the duration of 50% loss of xylem conductivity, as well as the
503 maximum loss of xylem conductivity during the dry season. With a deep rooting strategy, the
504 difference in the percentage loss of xylem conductivity between safe stomatal and risky stomatal
505 cases increases with the progression of the drought, but with a shallow rooting strategy, this
506 difference remains more or less the same over time. In addition, in 2011, a very wet year, with
507 deep roots, a safe xylem strategy is able to maintain the maximum xylem conductivity even
508 during dry season (Fig 4a). The impact of xylem strategy on the percentage loss of xylem
509 conductivity is relatively weak. For both deep- and shallow-rooted cases, trees with safe xylem
510 lose less xylem conductivity during the wet season but lose more conductivity during the dry
511 season.

512 The safe stomata & safe xylem cases for both deep- and shallow-rooted trees experience
513 greater declines in stem conductivity as compared to the safe stomata and efficient xylem for the
514 corresponding rooting depths (Fig. 4a). This is because with safe stomata, trees operate at the
515 right end of the vulnerability curve shown in fig. 1b, where the hydraulic conductivity of
516 efficient xylem is much higher than that of the safe xylem. Thus, when transpiring the same
517 amount of water, the efficient xylem will lose less water potential as compared to safe xylem.
518 This keeps the xylem water potential of a plant with efficient xylem higher than one with safe
519 xylem, and consequently also keeps the xylem conductivity, K, higher. This is also because we
520 set $P50_{gs}$ based on P_{xylem}, thus the $P50_{gs}$ of safe stomata for plants with efficient xylem is higher
521 (less negative) than that of plants with safe xylem, thus resulting in lower transpiration rates,
522 which in term reduces the loss of xylem water potential. As a result, plants with both safe
523 stomata and efficient xylem not only transpire less water but also lose less water potential per
524 volume of water transpired. Together, these two mechanisms contribute to keep the xylem
525 conductivity of the efficient xylem cases higher.

526   Stomatal, rooting, and xylem strategies have similar impacts on the seasonal variation of

527   both leaf and fine root water potentials (Fig4c and 4d). Leaf and fine root water potentials peak

528   during the winter, then start to decline in early spring, and reach their lowest point in the dry

529   season. Deep roots, safe stomata, and safe xylem traits all contribute to the maintenance of

530   higher leaf and fine root water potentials during the growing and dry seasons. With deep roots,

531   there is less difference in leaf and fine root water potential between stomatal and xylem

532   strategies in the very wet year 2011. Plants that combine safe stomata and/or safe xylem with

533   deep roots can keep the leaf and fine root water potentials relatively high (less than -5 Mpa)

534   during the dry season of the drought period. However, while plants that combine risky stomata or

535   efficient xylem with deep roots can keep the dry season leaf water potential above -5 Mpa during

536   the pre-drought period, their traits lead to the dry season leaf water potential dropping below -8

537   Mpa or even below -10 Mpa during the drought period. In both deep-rooted and shallow-rooted

538   cases, safe xylem leads to much lower leaf and fine root water potentials during the dry season.

539   The seasonal and inter-annual variation of fine root water potentials are almost identical to the

540   leaf water potential, except that the water potential of fine roots is slightly higher (~ 0.5 Mpa)

541   than the leaf water potential.

542

543   3.3 ~~Impact on~~Sensitivity of   subsurface hydrology to parameter perturbations

544   In the simulation outcomes, the vertical root distributions again have the largest impact on

545   hydrologic processes and subsurface water content and the way that they change over the

546   drought. With deep roots, there is less drainage loss from surface and subsurface runoff as

547   compared to shallow roots, especially during the growing season (Figure 5a,c,e,g). The

548   subsurface water content shows different vertical and temporal patterns between the cases with

549   different vertical root distributions. In the deep-rooted cases, during the pre-drought period, the

550   water content in the deepest layers fluctuates between wet and dry seasonally; during the first

551   year of the drought, the water content of the deepest layers (6 to 8m) slightly increases during the

552   wet season, but with the progression of the drought, the soil water content becomes consistently

553   depleted in the middle and deep layers (between 5 and 8 m depth) and only the shallow layer

554   (<0.16 m) water content increases during wet season. In the shallow-rooted cases (Figure

555   5b,d,f,h), soil moisture in the surface layers (top 2m) shows seasonal variation, but this seasonal

variation becomes weaker over depth and the soil moisture at 6-8m depth stays consistently high throughout the year during pre-drought period, and remains slightly low through the entire drought period; while the water content of the middle and upper layers of the shallow-rooted case have a similar pattern of seasonal variation before and during the drought.

Stomatal strategy, as quantified by $P50_{gs}$, has a weak impact on hydrologic processes and soil moisture. In both the deep- and shallow-rooted cases, riskier stomata lead to a slightly lower total subsurface water content (Figure 6a). The effect of $P50_{gs}$ is less significant during the pre-drought period for both the deep-rooted and shallow-rooted cases, and becomes more significant as the drought progresses. The effect of $P50_{gs}$ on total subsurface water content is less significant in shallow-rooted cases. Figure 5c shows the effect of $P50_{gs}$ on the water content of shallow and deep soil layers. In both the shallow- and deep-rooted cases, increasing $P50_{gs}$ has a negligible impact on the water content of the shallow layers during both the pre-drought and drought periods (Figure 5c left). For deeper layers, in the shallow-rooted case, $P50_{gs}$ has no impact on the water content at all times; in the deep-rooted cases, a risky $P50_{gs}$ results in lower dry season water content of deep layers (7-8m) during the pre-drought period (indicated by the red cycles of Figure 5a and 5c), but decreases the water content of those layers year round during the drought period (Figure 5a and 5e). In deep-rooted cases, safe stomata with efficient xylem lead to a slightly higher water content in deep layers (5m to 8m) during the pre-drought period, and in shallow layers (0 to 3m) during the drought period (Figure 6a). Risky stomata with safe xylem in deep-rooted cases are most effective in accessing soil water. Though the soil water contents are generally high in shallow-rooted cases, stomatal and xylem strategies show a similar impact on the soil water storage as those in the deep-rooted cases (Fig S4).

Simulations with deep roots have almost no loss of soil water to drainage during the dry season in normal years, or during the whole drought period; while with shallow roots, the drainage loss is high during the pre-drought period and decreases through the drought period, but still with some runoff even at the end of the drought period (Figure 6a). The observed total annual runoff from the 2008 to 2011 pre-drought period was about 250 mm/year, but was zero during the 2012 – 2015 drought period (from figure 4, Bales et al. 2018). This observed difference in runoff between the pre-drought (~290mm/year, 2011 - 2012) and drought periods (~0 mm/year) from the deep-rooted case is consistent with the predicted pattern. During the pre-

586 drought period, the wet season total subsurface water contents from Dec. to Feb. are similar
587 between the cases with deep and shallow roots, but during the dry season (from June to Sep.) the
588 total subsurface water content with shallow roots is substantially higher than the case with deep
589 roots (Figure 6b).

590 **4. Discussion**

591 4.1 Vertical root distribution as the first order control

592   The outcome of our simulations indicates that the vertical root distribution exerts the first
593 order control over both ecosystem level fluxes and plant physiology at CZ2. This dominance of
594 rooting strategy over other hydraulic traits is related to the nature of the rainfall pattern of the
595 Mediterranean-type climate of that region. The CZ2 site receives effectively all of its rain during
596 winter. This water is stored in the soil column and slowly released through the growing season.
597 The root zone soil moisture has strong seasonal variation, which constrains plant water use and
598 gas exchange as a function of the gradual drying of the soil column (Bales et al., 2018). In the
599 model, the stomatal behavior is controlled by the leaf water potential, which itself is strongly
600 affected by the root zone soil moisture. In our simulations, the daytime average leaf water
601 potential of a 55cm DBH cohort is well correlated with the fine root water potential and is
602 always about 0.5 Mpa lower (fig S5). This offset is consistent with the relationship between mid-
603 day leaf water potential and pre-dawn leaf water potential found by Martínez-Vilalta et al. (2014)
604 at the global scale.

605   With deep roots, trees use more subsurface storage capacity at the CZ2 site, and thus a
606 higher amount of total rainfall. In a wet year such as 2011, the root zone water potential of deep-
607 rooted trees is kept relatively high (Figure 4b) and the trees operate at the upper end of their
608 vulnerability curve through the year, with typical loss of conductivity < 10% (Fig 7). Therefore,
609 we don't see much effect of the stomatal strategy on GPP and transpiration in a wet year. At the
610 upper end of the vulnerability curve, stomata are fully open regardless of the stomatal strategy
611 (either to be safe or risky). When the drought began in late 2012, annual rainfall fell below the
612 total root zone storage, thus the deep storage remained depleted throughout the year. During the
613 drought, the deep-rooted trees were able to operate at the high end of the vulnerability curve in
614 the wet season, when the rainfall recharged the surface layer. As the surface layers dry, water

615 ~~potentials~~potential   then gradually falls to the lower end of the vulnerability curve;

616 consequently the photosynthesis and transpiration start to drop as the dry season progresses.

617 With risky stomata, trees can drive the soil moisture ~~a little further down.~~to lower values   . This

618 is why we see the difference in the effect on GPP and transpiration between different stomatal

619 strategies during the dry season when the drought progresses.

620   With shallow roots, trees can only use surface soil moisture storage. As a result, the

621 surface water storage is quickly used up after the wet season, and the root zone water potential

622 drops near the low end of the vulnerability curve during the dry season. Thus, the shallow-rooted

623 trees operate along the full extent of the vulnerability curve year-round, both during the pre-

624 drought and drought periods. Therefore, as for the deep-rooted cases, we don't see a strong effect

625 of stomatal strategy on GPP and transpiration during the wet season, but unlike the deep root

626 cases, the effect of stomatal strategy on GPP and transpiration during the dry season can be seen

627 throughout the whole simulation period.

628   Rooting strategies greatly control the spatial pattern of vertical soil water content (Figure

629 5). With deep roots, the vertical soil moisture variation is more homogeneous due to the

630 extensive root distribution. With shallow roots, the soil becomes extremely dry at the surface

631 (<1m) and extremely wet in deep layers (>5m) resulting from the aggregated root distribution

632 ~~at~~in the   upper layers. Our finding is similar to a recent study conducted by Agee et al. (2021),

633 where the authors found that the extensive lateral root spreading results in homogeneous soil

634 moisture distribution. The homogeneous soil moisture pattern may contribute to a more energy

635 efficient system that reduces plant water stress (Agee et al. 2021) because that minimizes the

636 energy dissipation loss through water transport (Hildebrandt et al. 2016). Both Agee et al (2021)

637 and our studies emphasize the importance of the means by which the root distributions determine

638 how the subsurface storage is utilized.

639   Given the shape of the vulnerability curves, in all these simulations, plants will stop

640 transpiring when their leaf water potential reaches around -10Mpa with efficient xylem or -

641 15Mpa with safe xylem, depending on their stomatal strategy (Fig 7). Because we are here

642 holding the stand structure and leaf area constant to allow comparison between cases, the

643 simulated leaf water potential of the shallow rooted, risky stomata combination can get as low as

644 -15Mpa (Figure 4b) during dry seasons even during pre-drought period, which is well below the

645 lowest possible leaf water potential observed (-10Mpa) (Vesala et al., 2017). Leaves will likely

646 be wilted before the water potential drops below -10Mpa and the tree would have already shed

647 the leaves due to canopy desiccation. But we specifically do not permit that to occur in these

648 simulations, so as to keep the different cases comparable. Although it might be unrealistic, the

649 leaf water potential can serve as an ~~indicate~~indicator of the degree of canopy desiccation. With

650 no or very little ~~leaf~~leaves, trees would rely on the storage carbon to support respiratory

651 demand until the wet season comes to regrow leaves.- Depending on the duration of the dry

652 season, trees may exhaust the stored carbon and die from carbon starvation.- Risky stomata

653 can generate higher GPP (Figure 1a), but also result in longer duration of more negative leaf

654 water potential (Figure 4b). This suggests that shallow rooted pines at CZ2 with risky stomata

655 will benefit from allocating more net primary productivity to their storage pools rather than

656 growth in order to reduce the carbon-starvation mortality. Therefore, even though the model

657 generates unrealistically low leaf water potentials, the extent and the duration of the simulated

658 very low leaf water potential allows us to gain some insight on the interaction of plant hydraulic

659 strategy and the life history strategy of conifer trees under a Mediterranean-type climate.

660 Further, the unrealistic leaf water potential from the shallow root simulations indicates that the

661 trees at that site must have really deep roots to exist at this site, which is in agreement with the

662 conclusions of Goulden and Bales (2019).

663   In this simulation, the impacts of xylem traits on GPP and ET are weak and subtle. This is

664 the result of the relative position of the two vulnerability curves, in particular, the intersection of

665 the two vulnerability curves in absolute conductivity. When the absolute conductivity is plotted

666 as a function of pressure (fig. 1b and solid lines in fig. S6), it can be seen that, on the left side of

667 the intersection, the safe xylem is not only safe but also efficient, and a safety-efficiency tradeoff

668 of xylem thus only occurs on the right side of the intersection point. Therefore, in shallow-rooted

669 cases, when the root zone water content—and hence plant water status—is low, safe xylem can

670 generate slightly higher GPP and ET than unsafe xylem. Furthermore, the two pressure-

671 conductivity curves diverge mainly at the wet end (corresponding to the wet season). This is

672 likely because the xylem structures of conifers are very similar, and the range of variation of

673 xylem traits in the sensitivity analysis are limited to the dominant species at the site. Therefore,

674 the difference in the xylem traits of conifers do not cause significant impacts on the ecosystem

675 level fluxes under the Mediterranean-type climate of CZ2, where the ecosystem fluxes are

676 constrained by energy during the wet season (Goulden et al., 2012). In addition, the maximum

677 rate of GPP and ET are co-constrained by the stand density, the total leaf area, the maximum

678 stomatal conductance, and VPD. In this study, we used the static stand structure mode of

679 FATES-Hydro, whereby the stand density and the total leaf biomass (so as total leaf area) of the

680 trees are held constant. This further limits the effect of xylem traits on GPP and ET.

681

682 4.2 Balancing productivity and mortality risk

683 The hydraulic traits that contribute to high carbon fixation rates often make trees more

684 susceptible to drought. Stomatal strategy ($P50_{gs}$) can have both positive and negative impact on

685 the trees, creating a tradeoff in the balance between productivity and physiological stress. The

686 risky stomata ($P50_{gs} = P50_x$) can generate higher GPP but also result in a greater loss of xylem

687 conductivity and lower leaf water potential. The tradeoff varies depending on the plant's root

688 strategy—i.e. having a deep vs. a shallow root distribution—and the moisture state.

689 To better understand the tradeoff between productivity and mortality risk, we plot the

690 simulated annual average GPP for each year against the fraction of conductivity (K/Kmax) of a

691 55cm DBH cohort for two scenarios: deep roots (Fig. 8a) and shallow roots (Fig. 8b), with

692 different combination of xylem and stomatal strategies. In both scenarios, for each pair of xylem

693 and stomatal strategies, the GPP per tree increases almost linearly with the K/Kmax. But, with

694 increasing the safety of the stomata, the GPP declines faster with loss of conductivity. This

695 response is stronger in deep-rooted scenarios. ~~Efficient~~Having e   fficient xylem only slightly

696 increases the steepness of the lines. The stomatal strategies thus represent points along a

697 gradient of the tradeoff between growth and mortality risk - the safer the stomata, the more GPP

698 is traded for reducing the mortality risk.

699 Along this tradeoff space, where trees can maximize their net carbon gains likely depends

700 on the xylem traits. Studies have shown that trees may temporarily lose xylem conductivity

701 during mild drought, which can recover once the soil water becomes available. However, under

702 an extreme drought, their xylem could collapse and permanently damage the xylem conduits. In

703 this case, trees rely on new sapwood growth to support the transpiration (Brodribb et al. 2010,

704 Anderegg et al. 2013). At one extreme, if the stomatal behavior is too safe, it will give low GPP

705 and the tree will be outcompeted for light due to faster-growing neighbors, but at the other

706 extreme, if the stomata behave very aggressive (risky), it will give high GPP but also empty the

707 subsurface storage quickly, consequently leading to a prolonged dry period of soil moisture. This

708 would lead to substantial xylem damage (and/or root death), and then the carbon needed to grow

709 new sapwood (or roots) can exceed the benefit of getting the additional GPP. So, the optimal

710 location along the gradient would probably be located slightly below the K/Kmax associated

711 with that critical xylem water potential. Currently, the xylem refilling and associated carbon cost

712 are not incorporated in ~~the~~ FATES-Hydro. These two processes should be implemented in the

713 model to better understand the water-carbon balance~~.~~, and thus remains as future work.

714 In the deep-rooted scenario, the values of the pre-drought period and early drought stage

715 are clustered at the upper-right corner, above K/Kmax of 0.6. (Fig. 8a). In this region, the stress

716 from the loss of xylem conductivity likely won't be high enough to cause severe consequences, if

717 using 50 percent loss of xylem conductivity as the threshold for mortality and/or permanent

718 xylem damage. The deep-rooted tree can thus benefit by trading less GPP for maintaining xylem

719 conductivity with a risky/more-productive stomatal strategy during normal years. But, during the

720 late stage of the drought (2014 and 2015), the conductivity values become much lower. If this

721 mega drought stopped earlier, e.g. if it were a mild drought that only lasted for two years, the

722 additional GPP obtained from risky stomata may overweight the carbon cost for repairing xylem

723 damage. This suggests that, if the 2012 – 2015 drought was not common in California, natural

724 selection might favor the risky/more-productive stomatal strategy for deep-rooted trees.

725 However, this same strategy also exposes trees to high mortality risk under severe droughts.

726 In the shallow-rooted case (Fig. 8b), the values are all clustered lower and to the left, as

727 compared to deep rooted scenario, irrespective of the drought status. Thus, for shallow roots,

728 risky/more-productive stomatal behavior results in a similarly high mortality risk during both the

729 pre-drought and drought period. Thus, under the long-term climate conditions seen at CZ2,

730 whether or not severe droughts were frequent, the only shallow-rooted trees that could persist

731 would have to follow the safe and less-productive stomatal strategy. And, ~~this~~thus safe and

732 less-productive stomata also protects the shallow-rooted tree plant from mortality risk during

733 drought.

The model outcome indicates that under drier root zone soil conditions, if pines were to follow a shallow rooting strategy, they would benefit from a safer stomatal strategy, with more conservative water use; but if they follow a deep rooting strategy, pines would benefit from riskier stomata. This is consistent with Anderegg et al.'s (2016) finding on the relative stomatal conductance (gs) across elevation. They found that at low elevation (lower precipitation) site, Ponderosa pine has lower relative stomatal conductance and less loss of %__xylem conductivity, equivalent to safer stomata in our study, while at mid elevation (higher precipitation) site, pine has higher relative stomatal conductance and moregreater__ loss of %__xylem conductivity, equivalent to risky stomata in our study. The simulation results are consistent with the idea that the CZ2 region is dominated by deep-rooted trees. This is supported by previous studies. In situ measurements of regolith structure (particularly the porosity) indicates that at CZ2, there is a layer of thick semi-weathered bed-__rock that allows the trees to grow deep roots (Holbrook et al., 2014). Growing deep roots to access rock moisture to support plant water use has also been observed in the Eel River CZO catchment (Rempe et al., 2018), another Mediterranean-type ecosystem along the west coast. Observed net CO_2 exchange and ET during the pre-drought period suggest that during a wet year, deep moisture supported summer transpiration and productivity when the upper layer moisture was low (Goulden et al. 2015). Because the deep rooting strategy is sufficient in most cases to avoid the main effects of dry seasons and short droughts, and that, conditional on having deep roots, the risky stomatal strategy confers a productivity advantage at little increased risk of vulnerability, then we would expect that plants with these traits would dominate. However, under extreme cases such as the 2012 - 2015 drought, which ranked as one of the most severe in California in the last 1200 years (Lu et al. 2019), we would expect that plants with this deep-rooted, risky stomatal strategy would be highly vulnerable to drought, which is consistent with the ~90% mortality of the pine observed at CZ2 during the drought (Fettig et al. 2019). The water balance of the catchment based on the long-term observation from precipitation, stream flow, and ET (Bales et al. 2018, Goulden and Bales 2019) also support that it was the slow depletion of deep moisture that caused tree mortality in the late stage of the prolonged 2012 – 2015 drought.

The finding of our study indicates that the future drought mortality would likely occur in the ecosystems which are co-limited by water and other factors. In those ecosystems, trees can benefit from having more efficient but less safe hydraulic traits, which allow them to be more

competitive for water, and bring in higher GPP. The extra carbon gain can be used to develop measures to deal with other constraining factors, such as increase storage carbon to lower the risk of carbon starvation, or build thicker bark to resist fire, and to grow more roots which further enhance their capacity to compete for water.

5. Conclusions

Our analysis indicates that, in root distribution can affect the most competitive stomatal traits. In a Mediterranean-type climate where the supply of energy and water is desynchronized and accessible subsurface water storage capacity is close to annual precipitation, deep roots combined with risky stomata represent a beneficial strategy for high productivity in normal years with low mortality risk, but exposes trees to high mortality risk during multi-year droughts. While such a strategy enables trees to fully utilize subsurface storage and precipitation for productivity over the regular years, the lack of deep water storage recharge during droughts exposes trees to high drought stress and makes this strategy unfavorable under severe and prolonged drought. In contrast, shallow roots combined with safe stomata represent a strategy for drought resistance, albeit at the cost of considerably reduced productivity, as such a combination only allows trees to use shallow subsurface storage while leaving deep moisture untouched, thus less precipitation is used for productivity. But this strategy leaves trees to be less susceptible to drought-induced mortality should the deep reservoir be depleted. In contrast, shallow roots with risky stomata leads to high mortality even during non-drought years, thus an uncompetitive combination at the site. These results suggest that stomatal strategy is controlled by root zone soil moisture and regulated by root distribution in that region. Thus, our study underscores the importance of considering plant rooting and hydraulic strategies within the larger context of plant ecological strategies.

Author contribution

JD and CDK design the study and write the MS. JD conducted the simulation. PB, RB, MG provided model input data. BC, CDK, RF, RK, CX, and JD wrote the code. PB, RB, BC, RF, MG, RK, LK, JS, CX edited the MS. CDK provided the funding

Acknowledgement

795 We acknowledge support by the Director, Office of Science, Office of Biological and
796 Environmental Research of the U. S. Department of Energy under Contract DE-AC02-
797 05CH11231 through the Early Career Research Program, the University of California Laboratory
798 Fees Research Program, and National Science Foundation Southern Sierra Critical Zone
799 Observatory grant EAR-1331931. RF acknowledges funding by the European Union's Horizon
800 2020 (H2020) research and innovation program under Grant Agreement No. 101003536
801 (ESM2025 – Earth System Models for the Future) and 821003 (4C, Climate-Carbon Interactions
802 in the Coming Century)

803 **Data availability statement**

804 The FATES code (branch FATEScodeforMS1), parameter files and data that support the
805 findings of this study are openly available at ZENODO:
806 ~~https://zenodo.org/account/settings/github/repository/JunyanDing/Rooting-and-Hydraulic-~~
807 ~~strategy-of-pine-at-Sierra-CZ2-~~
808 https://zenodo.org/account/settings/github/repository/JunyanDing/Rooting-and-Hydraulic-
809 strategy-of-pine-at-Sierra-CZ2- (~~DOI 10.5281/zenodo.5504405).~~DOI 10.5281/zenodo.5504405).
810 The flux tower data can be retrieved from the UC Merced online database
811 (~~https://www.ess.uci.edu/~california/).~~https://www.ess.uci.edu/~california/).

812 **Competing interests**

813 The authors declare no conflict of interest

5. References

Abatzoglou J.T. and Brown T.J. "A comparison of statistical downscaling methods suited for wildfire applications" International Journal of Climatology (2012), 32, 772-780. 2012.

Adams, H. D. et al. "Mechanisms in Drought-Induced Tree Mortality." *Nature Ecology & Evolution* 1(September). http://dx.doi.org/10.1038/s41559-017-0248-x. 2017.

Agee, E., He, L., Bisht, G., Couvreur, V., Shahbaz, P., Meunier, F. et al., 2021. Root lateral interactions drive water uptake patterns under water limitation. Adv. Water Resour., 151: 103896.

Anderegg, W.R., Plavcová, L., Anderegg, L.D., Hacke, U.G., Berry, J.A. and Field, C.B., Drought's legacy: multiyear hydraulic deterioration underlies widespread aspen forest die-off and portends increased future risk. Global change biology, 19(4), pp.1188-1196. 2013.

Anderegg, L. D. L. and Hillerislambers, J. Drought stress limits the geographic ranges of two tree species via different physiological mechanisms Glob. Chang. Biol. 22 1029–45 Online: http://dx.doi.org/10.1111/gcb.13148 http://dx.doi.org/10.1111/gcb.13148 . 2016

Ando, Eigo, and Kinoshita, Toshinori. "Red Light-Induced Phosphorylation of Plasma Membrane H+ -ATPase in Stomatal Guard Cells." *Plant Physiology* 178(October): 838–49. 2018.

Baker, Kathryn V., Tai, Xiaonan, Miller, Megan L, Johnson, D. M., Six co-occurring conifer species in northern Idaho exhibit a continuum of hydraulic strategies during an extreme drought year, AoB PLANTS, Volume 11, Issue 5, October 2019, plz056,

Bales, Roger et al. "Spatially Distributed Water-Balance and Meteorological Data from the Rain – Snow Transition , Southern Sierra Nevada , California." : 1795–1805. 2018.

Bales, Roger et al. 2018. "Mechanisms Controlling the Impact of Multi-Year Drought on Mountain Hydrology." *Scientific Reports* (December 2017): 1–8.

Ball, J. Timothy, Ian E. Woodrow, and Joseph A. Berry. "A model predicting stomatal conductance and its contribution to the control of photosynthesis under different environmental conditions." Progress in photosynthesis research. Springer, Dordrecht, 221-224. 1987.

Barnard, DM, Meinzer, FC, Lachenbruch, B., McCulloh, KA, Johnson, DM, Woodruff, D.R. Climate-related trends in sapwood biophysical properties in two conifers: avoidance of hydraulic dysfunction through coordinated adjustments in xylem efficiency, safety and capacitance. Plant Cell Environ. Apr;34(4):643-54. doi: 10.1111/j.1365-3040.2010.02269.x. Epub 2011 Feb 11. PMID: 21309793. 2011

Bartlett, M.K., Klein, T., Jansen, S., Choat, B. and Sack, L., The correlations and sequence of plant stomatal, hydraulic, and wilting responses to drought. Proceedings of the National Academy of Sciences, 113(46), pp.13098-13103. 2016.

Brodribb, T.J., Bowman, D.J., Nichols, S., Delzon, S. and Burlett, R., 2010. Xylem function and growth rate interact to determine recovery rates after exposure to extreme water deficit. New Phytologist, 188(2), pp.533-542.

Buotte, Polly C., Samuel Levis, Beverly E. Law, Tara W. Hudiburg, David E. Rupp, and Jeffery J. Kent. "Near - Future Forest Vulnerability to Drought and Fire Varies across the Western United States." (July):1–14. 2018.

Canadell, J.G., Le Quéré, C., Raupach, M.R., Field, C.B., Buitenhuis, E.T., Ciais, P., Conway, T.J., Gillett, N.P., Houghton, R.A. and Marland, G., Contributions to accelerating atmospheric CO2 growth from economic activity, carbon intensity, and efficiency of natural sinks. *Proceedings of the national academy of sciences*, *104*(47), pp.18866-18870. 2007.

Choat, Brendan, and Jarmila Pittermann. "New Insights into Bordered Pit Structure and Cavitation Resistance in Angiosperms and Conifers." *New Phytologist*: 555–57. 2009.

Christoffersen, B. O. et al. "Linking Hydraulic Traits to Tropical Forest Function in a Size-Structured and Trait-Driven Model (TFS v . 1-Hydro)." : 4227–55. 2016.

Coley, P.D., Bryant, J.P. and Chapin, F.S., Resource availability and plant antiherbivore defense. *Science*, *230*(4728), pp.895-899. 1985.

Corcuera, L., Cochard, H., Gil-Pelegrin, E. and Notivol, E., Phenotypic plasticity in mesic populations of Pinus pinaster improves resistance to xylem embolism (P 50) under severe drought. Trees, 25(6), pp.1033-1042. 2011.

Craine, J.M., Tilman, D., Wedin, D., Reich, P., Tjoelker, M. and Knops, J., Functional traits, productivity and effects on nitrogen cycling of 33 grassland species. *Functional Ecology*, *16*(5), pp.563-574. 2002.

Danabasoglu, G. et al. "The Community Earth System Model Version 2 (CESM2) Journal of Advances in Modeling Earth Systems." *Journal of Advances in Modeling Earth Systems* 2: 1–35. 2020.

Domec, JC., Warren, J.M., Meinzer, F.C. *et al.* Native root xylem embolism and stomatal closure in stands of Douglas-fir and ponderosa pine: mitigation by hydraulic redistribution. *Oecologia* **141,** 7–16 https://doi.org/10.1007/s00442-004-1621-4.https://doi.org/10.1007/s00442-004-1621-4. 2004.

Fettig, Christopher J, Leif A Mortenson, M Bu, and Patra B Fou. "Tree Mortality Following Drought in the Central and Southern Sierra Nevada, California, U.S." *Forest Ecology and Management* 432: 164–78. 2019.

Fisher, R. a. et al. "Taking off the Training Wheels: The Properties of a Dynamic Vegetation Model without Climate Envelopes, CLM4.5(ED)." *Geoscientific Model Development* 8(11): 3593–3619. 2015.

Gaylord, M.L., Kolb, T.E. and McDowell, N.G.,. Mechanisms of piñon pine mortality after severe drought: a retrospective study of mature trees. *Tree physiology*, *35*(8), pp.806-816. 2015

Geen, Anthony Toby O et al. "Southern Sierra Critical Zone Observatory and Kings River Experimental Watersheds : A Synthesis of Measurements , New Insights , and Future Directions." *Vadose Zone J. Advancing Critical Zone ScienceAdvancing Critical Zone Science*. 2018.

Gleason, Sean M., Mark Westoby, Steven Jansen, Brendan Choat, Uwe G. Hacke, Robert B. Pratt, Radika Bhaskar, Tim J. Brodribb, Sandra J. Bucci, Kun Fang Cao, Hervé Cochard, Sylvain Delzon, Jean Christophe Domec, Ze Xin Fan, Taylor S. Feild, Anna L. Jacobsen, Daniel M. Johnson, Frederic Lens, Hafiz Maherali, Jordi Martínez-Vilalta, Stefan Mayr, Katherine A. Mcculloh, Maurizio Mencuccini, Patrick J. Mitchell, Hugh Morris, Andrea Nardini, Jarmila Pittermann, Lenka Plavcová, Stefan G. Schreiber, John S. Sperry, Ian J. Wright, and Amy E. Zanne. "Weak Tradeoff between Xylem Safety and Xylem-Specific Hydraulic Efficiency across the World's Woody Plant Species." *New Phytologist* 209(1):123–36. 2016.

Golaz, Jean-Christophe, Luke P. Van Roekel, Xue Zheng, Andrew F. Roberts, Jonathan D. Wolfe, Wuyin Lin, Andrew M. Bradley et al. "The DOE E3SM Model Version 2: overview of the physical model and initial model evaluation." Journal of Advances in Modeling Earth Systems 14, no. 12 (2022).

Goulden, M L et al. "Evapotranspiration along an Elevation Gradient in California ' s Sierra Nevada." *Journal of Geophysical Research* 117(1): 1–13. 2015.

Goulden, M L, and R C Bales. 2019. "California Forest Die-off Linked to Multi-Year Deep Soil Drying in 2012–2015 Drought." *Nature Geoscience* 12(August). http://dx.doi.org/10.1038/s41561-019-0388-5.

Grime, J.P., Evidence for the existence of three primary strategies in plants and its relevance to ecological and evolutionary theory. *The American Naturalist*, *111*(982), pp.1169-1194. 1977.

Grime, J.P., Plant strategies and vegetation processes. *Plant strategies and vegetation processes.* 1979.

Hacke, Uwe G., Rachel Spicer, Stefan G. Schreiber, and Lenka Plavcová. "An Ecophysiological and Developmental Perspective on Variation in Vessel Diameter." *Plant Cell and Environment* 40(6):831–45. 2017.

Hammond, W., K. Yu[+], L. Wilson, R. Will, W.R.L. Anderegg, and H. Adams. 2019. "Dead or dying? Quantifying the point of no return from hydraulic failure in drought-induced tree mortality". *New Phytologist*. doi: 10.1111/nph.15922. Published, 05/2019

Hartmann, Henrik, Waldemar Ziegler, Olaf Kolle, and Susan Trumbore. "Thirst Beats Hunger - Declining Hydration during Drought Prevents Carbon Starvation in Norway Spruce Saplings." *New Phytologist* 200(2):340–49. 2013.

Hartung, Wolfram, Angela Sauter, and Eleonore Hose. "Abscisic Acid in the Xylem : Where Does It Come from , Where Does It Go To ?" 53(366): 27–32. 2002.

Hetherington, Alistair M, and F Ian Woodward. "The Role of Stomata in Sensing and Driving Environmental Change." *Nature* 424(August): 901–8. 2003.

Huang, J., Kautz, M., Trowbridge, A. M., Hammerbacher, A., Raffa, K. F., Adams, H. D., ... & Gershenzon, J. Tree defence and bark beetles in a drying world: carbon partitioning, functioning and modelling. *New Phytologist*, *225*(1), 26-36. (2020).

Inouea, Shin-ichiro, and Toshinori Kinoshitaa. 2017. "Blue Light Regulation of Stomatal

932   Opening and the Plasma Membrane H+-ATPase 2." *Plant Physiology* (166): 17.

933 Ivanov, Valeriy Y., Lucy R. Hutyra, Steven C. Wofsy, J. William Munger, Scott R. Saleska,
934   Raimundo C. De Oliveira, and Plínio B. De Camargo. "Root Niche Separation Can Explain
935   Avoidance of Seasonal Drought Stress and Vulnerability of Overstory Trees to Extended
936   Drought in a Mature Amazonian Forest." *Water Resources Research* 48(12):1–21. 2012.

937 Jackson, R.B., Canadell, J., Ehleringer, J.R., Mooney, H.A., Sala, O.E. and Schulze, E.D., A
938   global analysis of root distributions for terrestrial biomes. *Oecologia*, *108*(3), pp.389-411.
939   1996.

940 Johnson, D. M., Domec, J. C., Carter Berry, Z., Schwantes, A. M., McCulloh, K. A., Woodruff,
941   D. R., ... & McDowell, N. G. Co-occurring woody species have diverse hydraulic strategies
942   and mortality rates during an extreme drought. *Plant, Cell & Environment*, *41*(3), 576-588.
943   2018.

944 Kattge, J., Bönisch, G., Díaz, S., Lavorel, S., Prentice, I. C., Leadley, P., Tautenhahn, S., Werner,
945   G., et al. "TRY Plant Trait Database - Enhanced Coverage and Open Access." *Global
946   Change Biology* 26(1):119–88. 2020.

947 Kelly, Anne E, and Michael L Goulden. "A Montane Mediterranean Climate Supports Year-
948   Round Photosynthesis and High Forest Biomass." : 459–68. 2016.

949 Khasanova, Albina, John T. Lovell, Jason Bonnette, Xiaoyu Weng, Jerry Jenkins, Yuko
950   Yoshinaga, Jeremy Schmutz, and Thomas E. Juenger. "The Genetic Architecture of Shoot
951   and Root Trait Divergence between Mesic and Xeric Ecotypes of a Perennial Grass."
952   *Frontiers in Plant Science* 10(April):1–10. 2019.

953 Kilgore, J.S., Jacobsen, A.L. and Telewski, F.W., Hydraulics of Pinus (subsection Ponderosae)
954   populations across an elevation gradient in the Santa Catalina Mountains of southern
955   Arizona. Madroño, 67(4), pp.218-226. 2021.

956 Klos, P Zion et al. "Subsurface Plant-Accessible Water in Mountain Ecosystems with a
957   Mediterranean Climate." *Wiley Interdisciplinary Reviews: Water* (May 2017): 1–14. 2017.

958 Koch, G.W. and Fredeen, A.L., Transport challenges in tall trees. In *Vascular transport in
959   plants* (pp. 437-456). Academic Press. 2005.

960 Koven, C.D., Knox, R.G., Fisher, R.A., Chambers, J.Q., Christoffersen, B.O., Davies, S.J.,
961   Detto, M., Dietze, M.C., Faybishenko, B., Holm, J. and Huang, M., Benchmarking and
962   parameter sensitivity of physiological and vegetation dynamics using the Functionally
963   Assembled Terrestrial Ecosystem Simulator (FATES) at Barro Colorado Island,
964   Panama. *Biogeosciences*, *17*(11), pp.3017-3044. 2020.

965 Kulmatiski, Andrew and Karen H. Beard. "Root Niche Partitioning among Grasses, Saplings,
966   and Trees Measured Using a Tracer Technique." *Oecologia* 171(1):25–37. 2013.

967 Lawrence, D.M., Fisher, R.A., Koven, C.D., Oleson, K.W., Swenson, S.C., Bonan, G., Collier,
968   N., Ghimire, B., van Kampenhout, L., Kennedy, D. and Kluzek, E., The Community Land
969   Model version 5: Description of new features, benchmarking, and impact of forcing
970   uncertainty. *Journal of Advances in Modeling Earth Systems*, *11*(12), pp.4245-4287.

Li, S., Lens, F., Espino, S., Karimi, Z., Klepsch, M., Schenk, H.J., Schmitt, M., Schuldt, B. and Jansen, S., 2016. Intervessel pit membrane thickness as a key determinant of embolism resistance in angiosperm xylem. *Iawa Journal*, *37*(2), pp.152-171. 2019.

Lu, Yaojie et al. 2019. "Optimal Stomatal Drought Response Shaped by Competition for Water and Hydraulic Risk Can Explain Plant Trait Covariation." (1977).

Mackay, D. S., Savoy, P. R., Grossiord, C., Tai, X., Pleban, J. R., Wang, D. R., ... & Sperry, J. S. Conifers depend on established roots during drought: results from a coupled model of carbon allocation and hydraulics. *New Phytologist*, *225*(2), 679-692. 2020.

Martínez-Vilalta, Jordi, Anna Sala, and Josep Piñol. *The Hydraulic Architecture of Pinaceae-a Review*. Vol. 171. 2004.

Matheny, Ashley M, Golnazalsadat Mirfenderesgi, and Gil Bohrer. "Trait-Based Representation of Hydrological Functional Properties of Plants in Weather and Ecosystem Models." *Plant Diversity* 39(1): 1–12. http://dx.doi.org/10.1016/j.pld.2016.10.001. 2017.

Matheny, A.M., Fiorella, R.P., Bohrer, G., Poulsen, C.J., Morin, T.H., Wunderlich, A., Vogel, C.S. and Curtis, P.S., Contrasting strategies of hydraulic control in two codominant temperate tree species. *Ecohydrology*, *10*(3), p.e1815. 2017.

Mcdowell, Nate, Nate Mcdowell, William T. Pockman, Craig D. Allen, D. David, Neil Cobb, Thomas Kolb, Jennifer Plaut, John Sperry, Adam West, David G. Williams, and Enrico A. Yepez. "Mechanisms of Plant Survival and Mortality during Drought : Why Do Some Plants Survive While Others Succumb To." 2008.

McDowell, Nate G. et al. "Evaluating Theories of Drought-Induced Vegetation Mortality Using a Multimodel – Experiment Framework." : 304–21. 2013.

Mooney, Harold and Erika Zavaleta. *Ecosystems of California*. Vol. 3. edited by H. Mooney and E. Zavaleta. Oakland, California, USA: Univ of California Press. 2003.

Mursinna, A. Rio, Erica McCormick, Kati Van Horn, Lisa Sartin, and Ashley M. Matheny. "Plant Hydraulic Trait Covariation: A Global Meta-Analysis to Reduce Degrees of Freedom in Trait-Based Hydrologic Models." *Forests* 9(8). 2018.

Oleson, Keith W et al. "Technical Description of Version 4.5 of the Community Land Model (CLM) Coordinating." In *Natl. Cent. Atmos. Res. Tech. Note*, Natl. Cent. for Atmos. Res., Boulder, Colo. 2013.

Pittermann, Jarmila, John S. Sperry, Uwe G. Hacke, James K. Wheeler, and Elzard H. Sikkema. "Inter-Tracheid Pitting and the Hydraulic Efficiency of Conifer Wood: The Role of Tracheid Allometry and Cavitation Protection." *American Journal of Botany* 93(9):1265–73. 2006.

Pittermann, Jarmila, John S. Sperry, James K. Wheeler, Uwe G. Hacke, and Elzard H. Sikkema. "Mechanical Reinforcement of Tracheids Compromises the Hydraulic Efficiency of Conifer Xylem." *Plant, Cell and Environment* 29(8):1618–28. 2006.

Pockman, W.T. and Sperry, J.S., Vulnerability to xylem cavitation and the distribution of Sonoran desert vegetation. *American journal of botany*, *87*(9), pp.1287-1299. 2000.

Powell, Thomas L., James K. Wheeler, Alex A. R. de Oliveira, Antonio Carlos Lola da Costa, Scott R. Saleska, Patrick Meir, and Paul R. Moorcroft. "Differences in Xylem and Leaf Hydraulic Traits Explain Differences in Drought Tolerance among Mature Amazon Rainforest Trees." *Global Change Biology* 23(10):4280–93. 2017.

Pratt, R.B. and Jacobsen, A.L., Conflicting demands on angiosperm xylem: tradeoffs among storage, transport and biomechanics. *Plant, Cell & Environment*, *40*(6), pp.897-913. 2017.

Reich, Peter B., Ian J. Wright, Jeannine Cavender-Bares, J. M. Craine, Jacek Oleksyn, M. Westoby, and M. B. Walters. "The evolution of plant functional variation: traits, spectra, and strategies." International Journal of Plant Sciences 164, no. S3: S143-S164. (2003).

Reichstein, M., Bahn, M., Mahecha, M.D., Kattge, J. and Baldocchi, D.D., Linking plant and ecosystem functional biogeography. *Proceedings of the National Academy of Sciences*, *111*(38), pp.13697-13702. 2014.

Rodriguez-Dominguez, C.M., Buckley, T.N., Egea, G., de Cires, A., Hernandez-Santana, V., Martorell, S. and Diaz-Espejo, A., Most stomatal closure in woody species under moderate drought can be explained by stomatal responses to leaf turgor. *Plant, Cell & Environment*, *39*(9), pp.2014-2026. 2016.

Rowland, L., A. C. L. Da Costa, D. R. Galbraith, R. S. Oliveira, O. J. Binks, A. A. R. Oliveira, A. M. Pullen, C. E. Doughty, D. B. Metcalfe, S. S. Vasconcelos, L. V. Ferreira, Y. Malhi, J. Grace, M. Mencuccini, and P. Meir. "Death from Drought in Tropical Forests Is Triggered by Hydraulics Not Carbon Starvation." *Nature* 528(7580):119–22. 2015.

Salmon, Yann, José M. Torres-Ruiz, Rafael Poyatos, Jordi Martinez-Vilalta, Patrick Meir, Hervé Cochard, and Maurizio Mencuccini. "Balancing the Risks of Hydraulic Failure and Carbon Starvation: A Twig Scale Analysis in Declining Scots Pine." *Plant Cell and Environment* 38(12):2575–88. 2015.

Sauter, Angela, W J Davies, Wolfram Hartung, and Lehrstuhl Botanik I. "The Long-Distance Abscisic Acid Signal in the Droughted Plant : The Fate of the Hormone on Its Way from Root to Shoot." 52(363): 1991–97. 2001.

Skelton, R. P., West, A. G., & Dawson, T. E. "Predicting plant vulnerability to drought in biodiverse regions using functional traits." *Proceedings of the National Academy of Sciences*, *112*(18), 5744-5749. 2015.

Sevanto, Sanna, Nate G. Mcdowell, L. Turin Dickman, Robert Pangle, and William T. Pockman. "How Do Trees Die? A Test of the Hydraulic Failure and Carbon Starvation Hypotheses." *Plant, Cell and Environment* 37(1):153–61. 2014.

Sperry, John S. "Evolution of Water Transport and Xylem Structure." *International Journal of Plant Sciences* 164. 2003.

Teuling, Adriaan J, Remko Uijlenhoet, and Peter A Troch. "Impact of Plant Water Uptake Strategy on Soil Moisture and Evapotranspiration Dynamics during Drydown." 33: 3–7. 2006.

Vesala, T., Sevanto, S., Grönholm, T., Salmon, Y., Nikinmaa, E., Hari, P. and Hölttä, T., Effect

of leaf water potential on internal humidity and CO2 dissolution: reverse transpiration and improved water use efficiency under negative pressure. *Frontiers in plant science*, *8*, p.54. 2017.

Westoby, M., Falster, D.S., Moles, A.T., Vesk, P.A. and Wright, I.J., Plant ecological strategies: some leading dimensions of variation between species. *Annual review of ecology and systematics*, *33*(1), pp.125-159. 2002.

Wilkinson, S, and W J Davies. "ABA-Based Chemical Signalling : The Co-Ordination Of." : 195–210. 2002.

Wullschleger, Stan D. et al. "Plant Functional Types in Earth System Models : Past Experiences and Future Directions for Application of Dynamic Vegetation Models in High-Latitude Ecosystems." *Annals of botany* (114): 1–16. 2014.

Yu, Gui-rui, Jie Zhuang, and Keiichi Nakayamma. "Root Water Uptake and Profile Soil Water as Affected by Vertical Root Distribution." *Plant Ecol*: 15–30. 2007.

Zeng, Xubin. "Global Vegetation Root Distribution for Land Modeling." *Journal of Hydrometeorology* 2(5): 525–30. 2001.

Tables

Table 1 Parameters used in FATES-Hydro sensitivity analysis

Parameters	Biological meaning	Values	Units
r_a, r_b	Root distribution: shallow roots vs. deep roots	(0.1, 0.1) – (2 5)	unitless
$P50_{gs}$	Leaf xylem water potential at half stomatal closure stomatal control on safety vs. efficiency	P50x – P20x	Mpa
$P50_x$	Xylem water potential when xylem loss half of the conductance	-3.0[a], -4.8[b]	Mpa
K_{max}	Maximum xylem conductivity per unit sap area	0.88[a], 0.64[b]	kg/MPa/m/s
A	Shape parameter of van Genuchten hydrologic function	0.11855[a], 0.088026[b]	Mpa^{-1}
m, n	Shape parameters of van Genuchten hydrologic function	(0.8, 1.25)[a], (0.8, 1.5)[b]	unitless

a: values for efficient/unsafe xylem
b: values for inefficient/safe xylem

Table 2. List of major parameters

Symbol	Source code name	Value	Units	Description	Source
a_{gs}	fates_hydr_avuln_gs	2.5	unitless	shape parameter for stomatal control of water vapor (slope)exiting leaf	Christoffersen et al., 2016
χ	fates_hydr_p_taper	0.333	unitless	xylem taper exponent	Christoffersen et al., 2016
$\pi_{o,l}$, $\pi_{o,s}$, $\pi_{o,r}$	fates_hydr_pinot_node	-1.47, -1.23, -1.04	MPa	osmotic potential at full turgor of leaf, stem, root	Christoffersen et al., 2016
$RWC_{res,l}$, $RWC_{res,s}$, $RWC_{res,r}$	fates_hydr_resid_node	0.25, 0.325, 0.15	proportion	residual fraction of leaf, stem, root	Christoffersen et al., 2016
$\Theta_{sat,x}$	fates_hydr_thetas_node	0.65	cm^3/cm^3	saturated water content of xylem	Christoffersen et al., 2016
SLA_{max}	fates_leaf_slamax	0.01	m^2/gC	Maximum Specific Leaf Area (SLA)	TRY
SLA_{top}	fates_leaf_slatop	0.01	m^2/gC	Specific Leaf Area (SLA) at top of canopy, projected area basis	TRY
$V_{cmax,25,\ top}$	fates_leaf_vcmax25top	55	umol CO2/m^2/s	maximum carboxylation rate of Rub. at 25C, canopy top	TRY
b_{opt} b_{opt}	fates_bbopt_c3	10000	umol H2O/m^2/s	Ball-Berry minimum leaf stomatal conductance for C3 plants	Calibrated

Figures

Figure 1
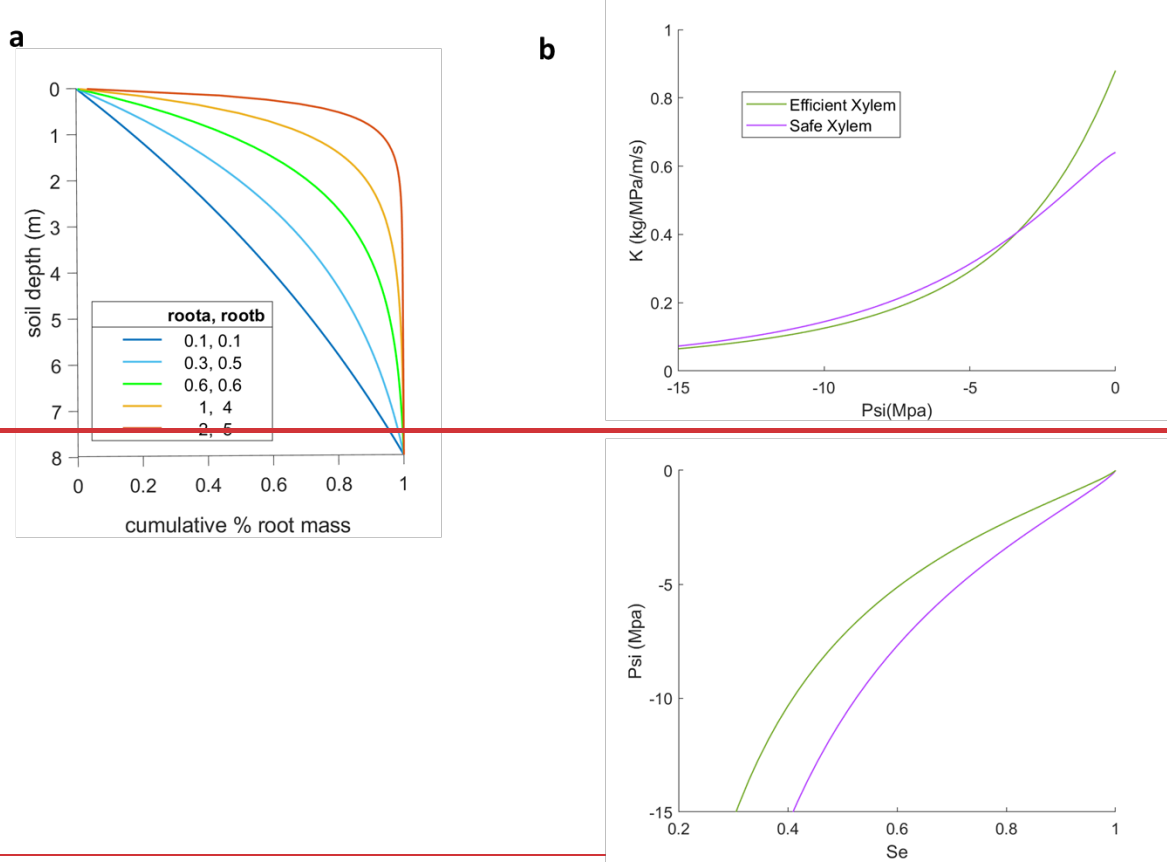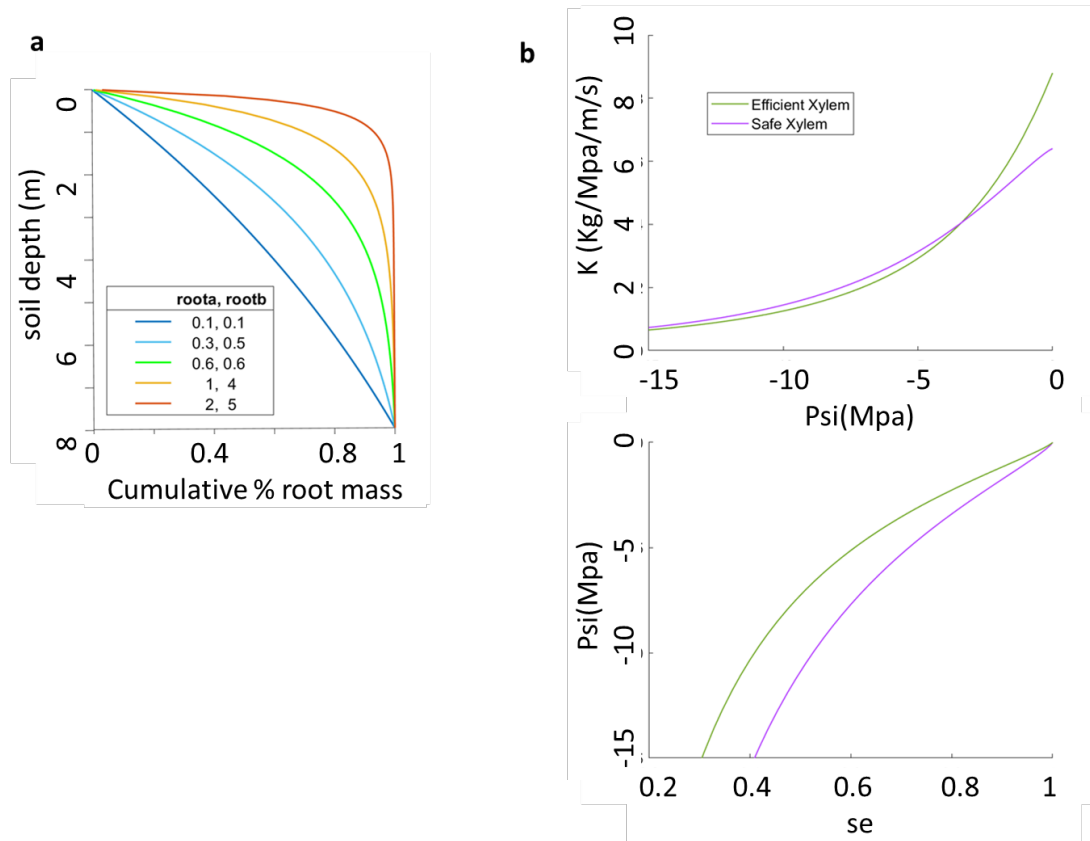
Figure 1. Sensitivity analysis set up for: a) root parameters that give five root distribution scenarios with effective rooting depths of 1m, 3m, 5m, 6.5m, and 8m , and b) two xylem scenarios for safe xylem (P50x=-4.8, Kmax=0.64), and efficient xylem (P50x=-2.5, Kmax=0.88).

Figure 2
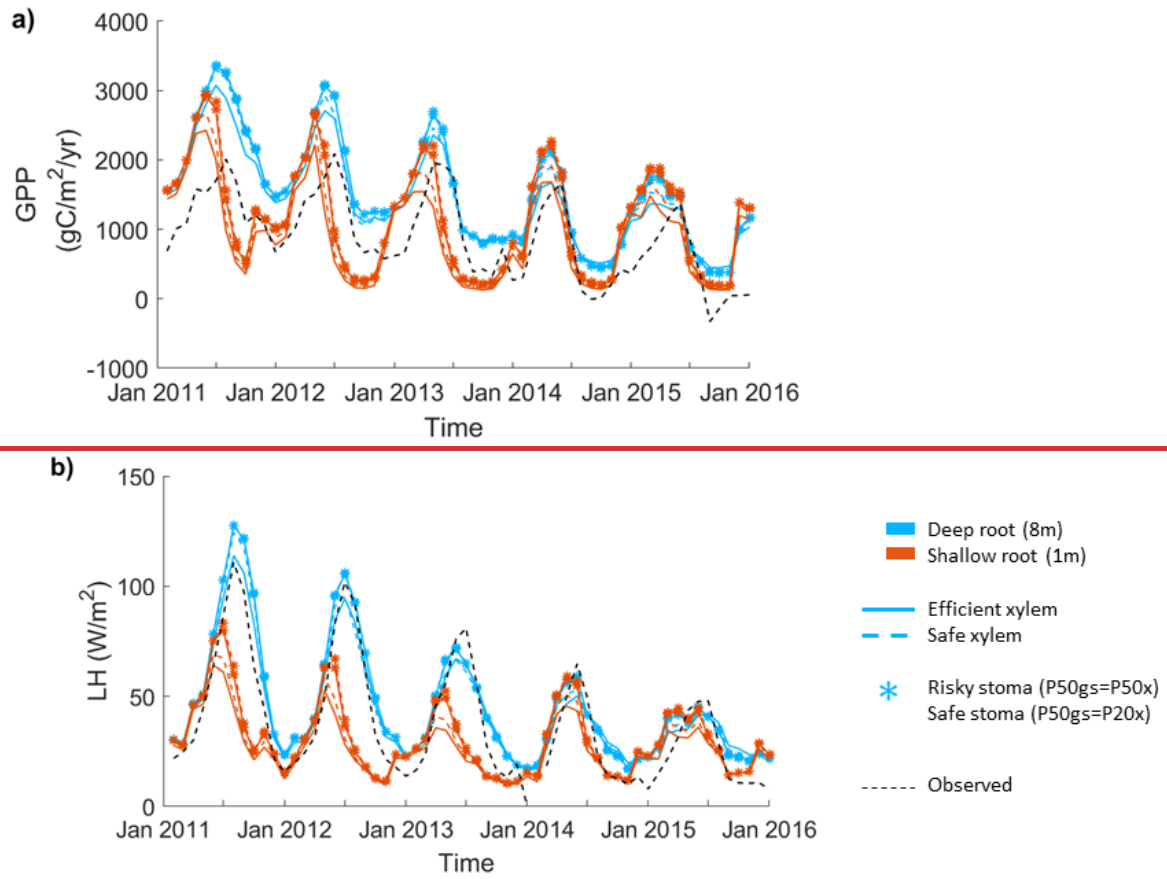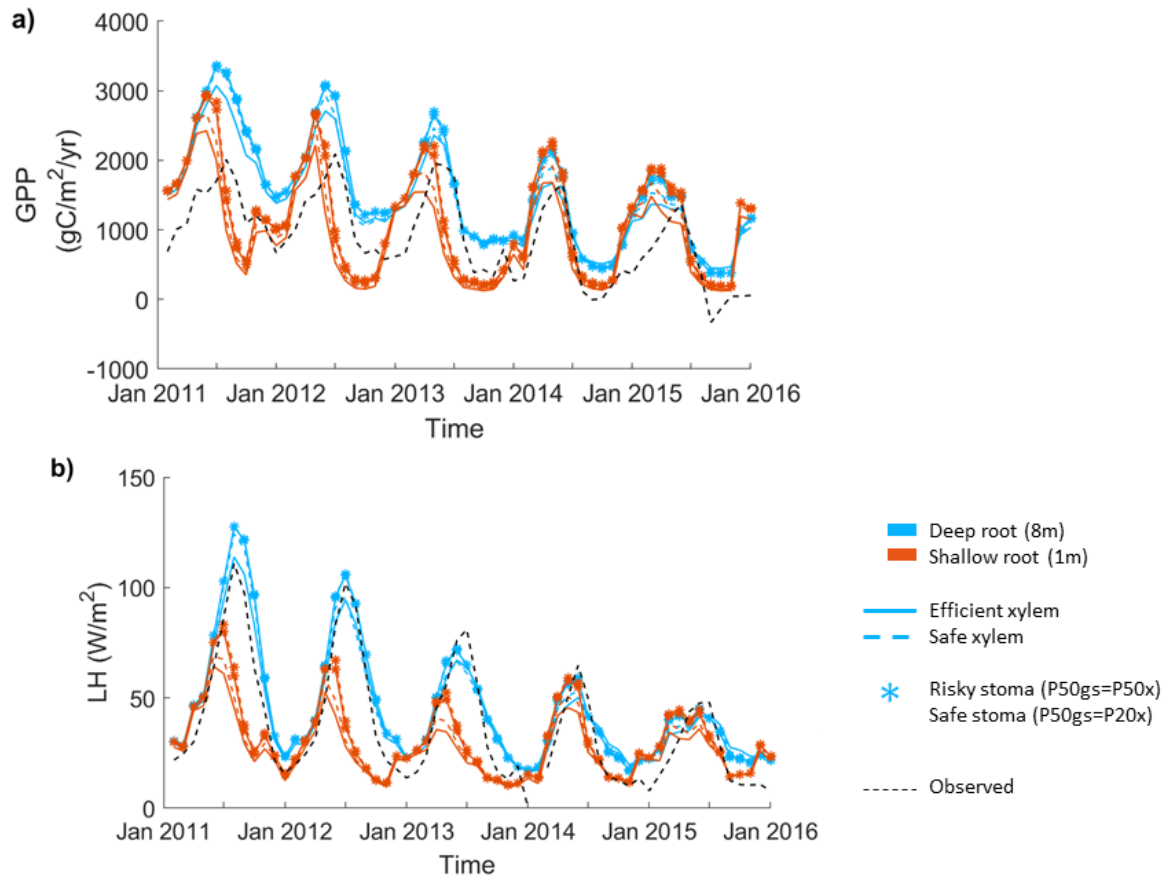
Figure 2. Impact of hydraulic strategies on ecosystem water and energy fluxes: a) monthly mean gross primary productivity, and B) monthly mean latent heat flux, of the end member cases.

Figure 3

Figure 3. Root mean square error of GPP (a-b), and latent heat flux (c-d) with respect to variation in input parameters.

Figure 4

fig4
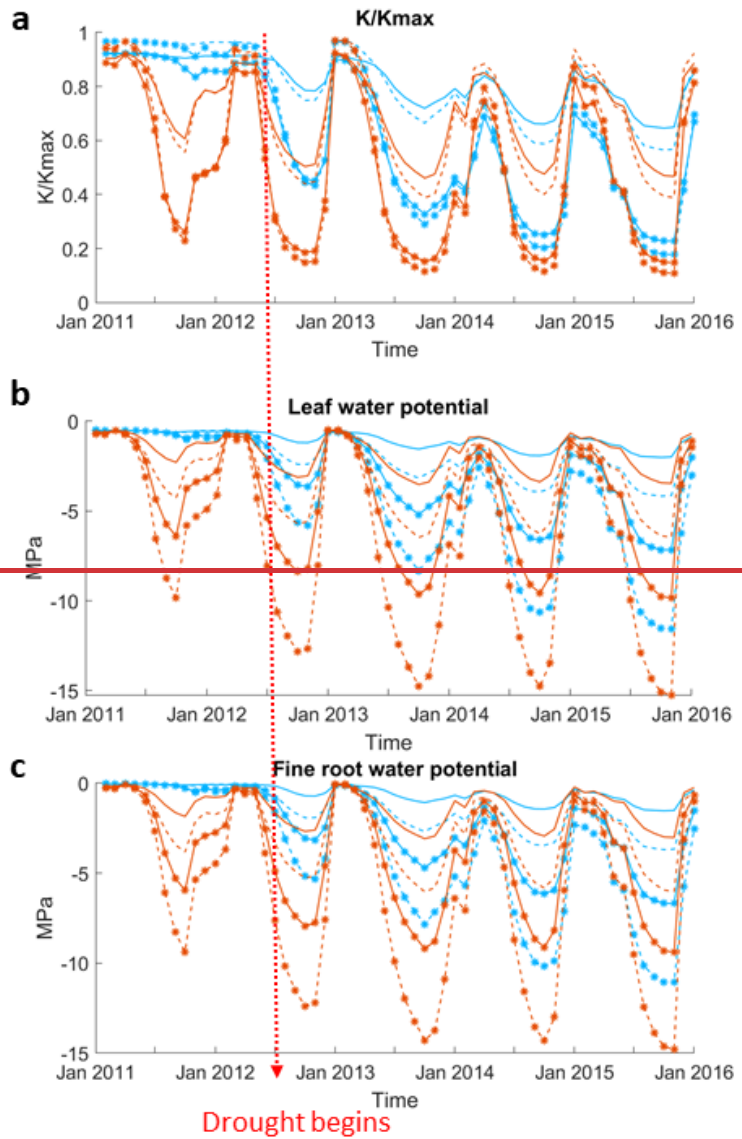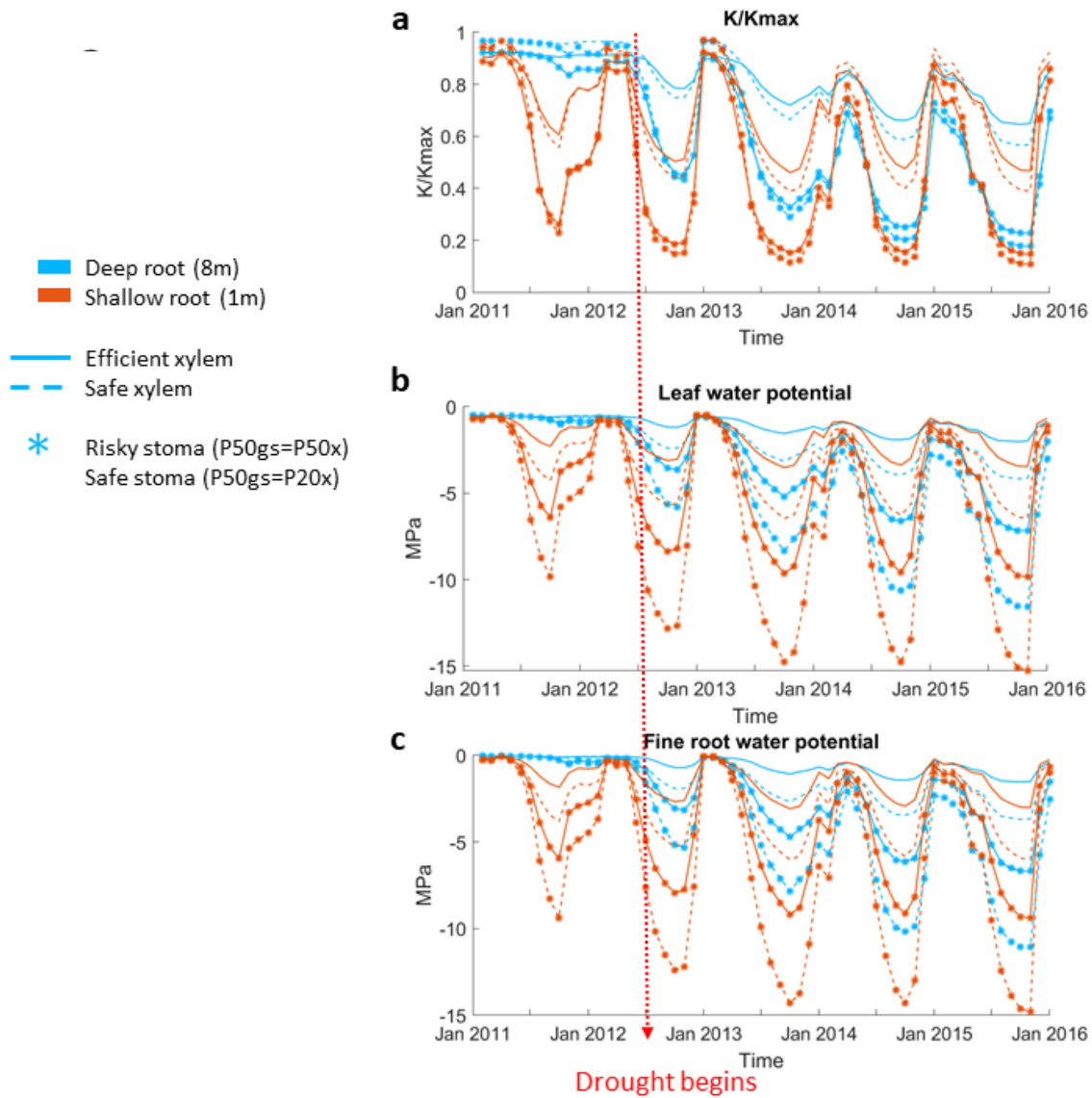
Figure 4. Seasonal and inter-annual variation of plant physiologic characteristics: a) monthly mean stem fraction of conductance K/K$_{max}$ (a), monthly mean leaf water potential, and c) monthly mean overall absorbing roots water potential, of the 55cm DBH cohort throughout the 2011-2015 period.

Figure 5
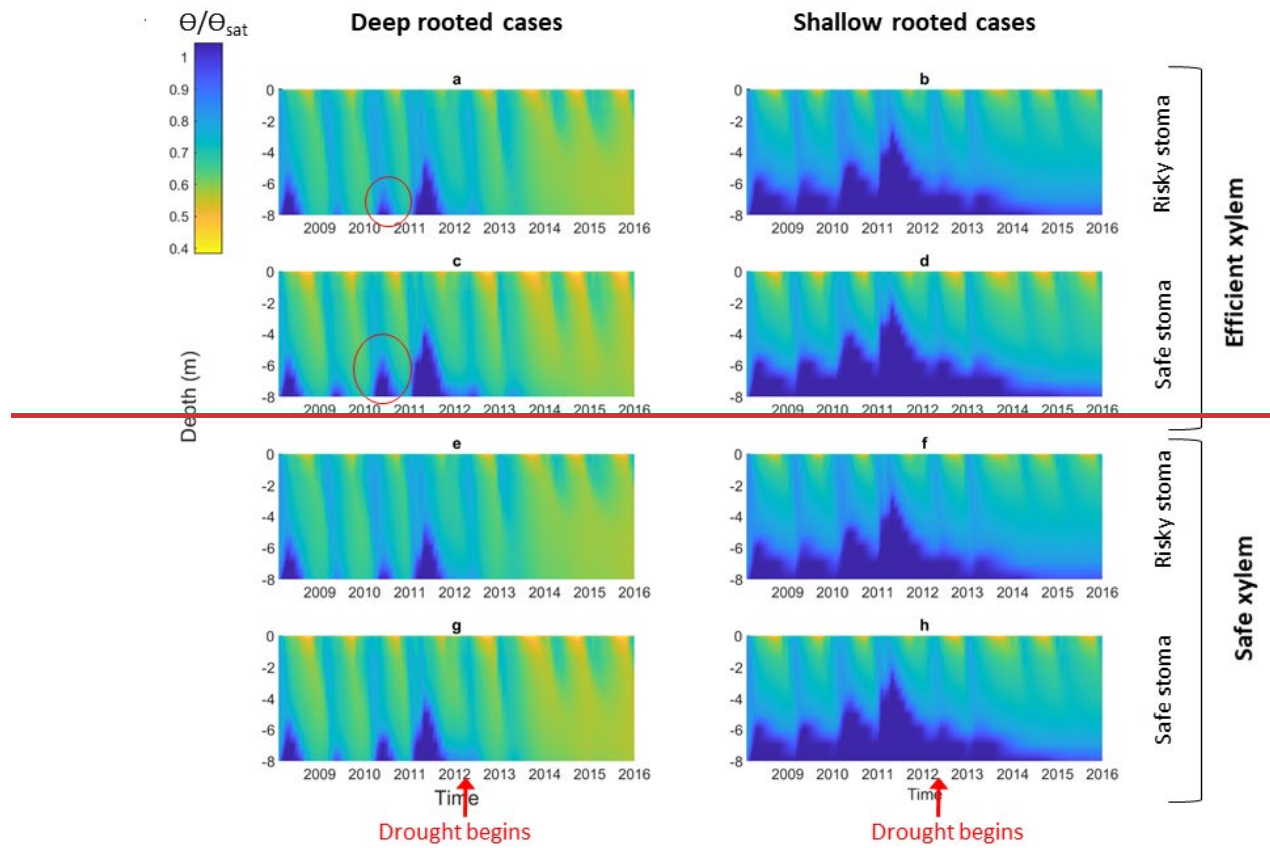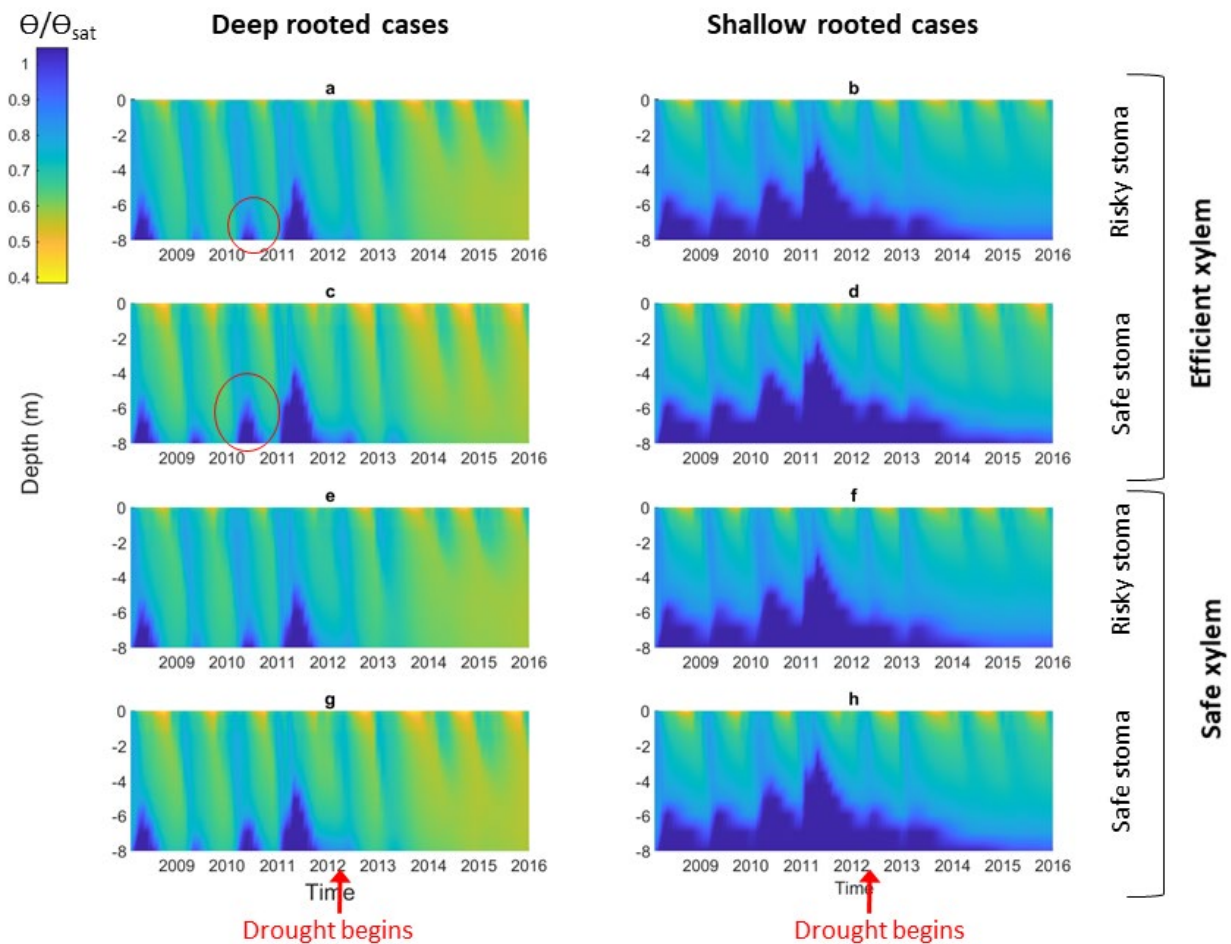
Figure 5. Impact of different combination of rooting depth, xylem and stomatal traits on soil moisture; left column shows deep rooted cases with a) efficient xylem and risky stoma, c) efficient xylem and safe stoma, e) safe xylem and risky stoma, g) safe xylem and safe stoma. Right column shows shallow rooted cases with b) efficient xylem and risky stoma, d) efficient xylem and safe stoma, f) safe xylem and risky stoma, h) safe xylem and safe stoma; red cycle highlights the effect of stomatal traits on deep water storage during the wet season of the pre-drought period
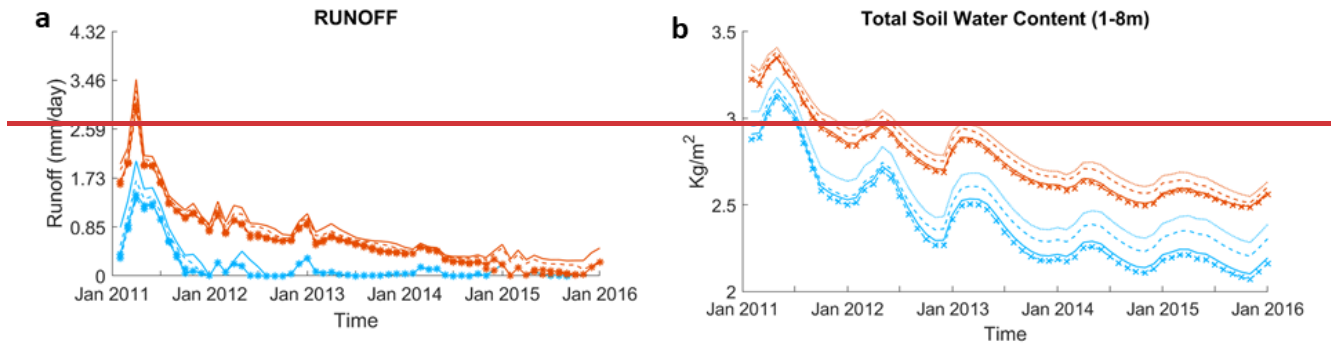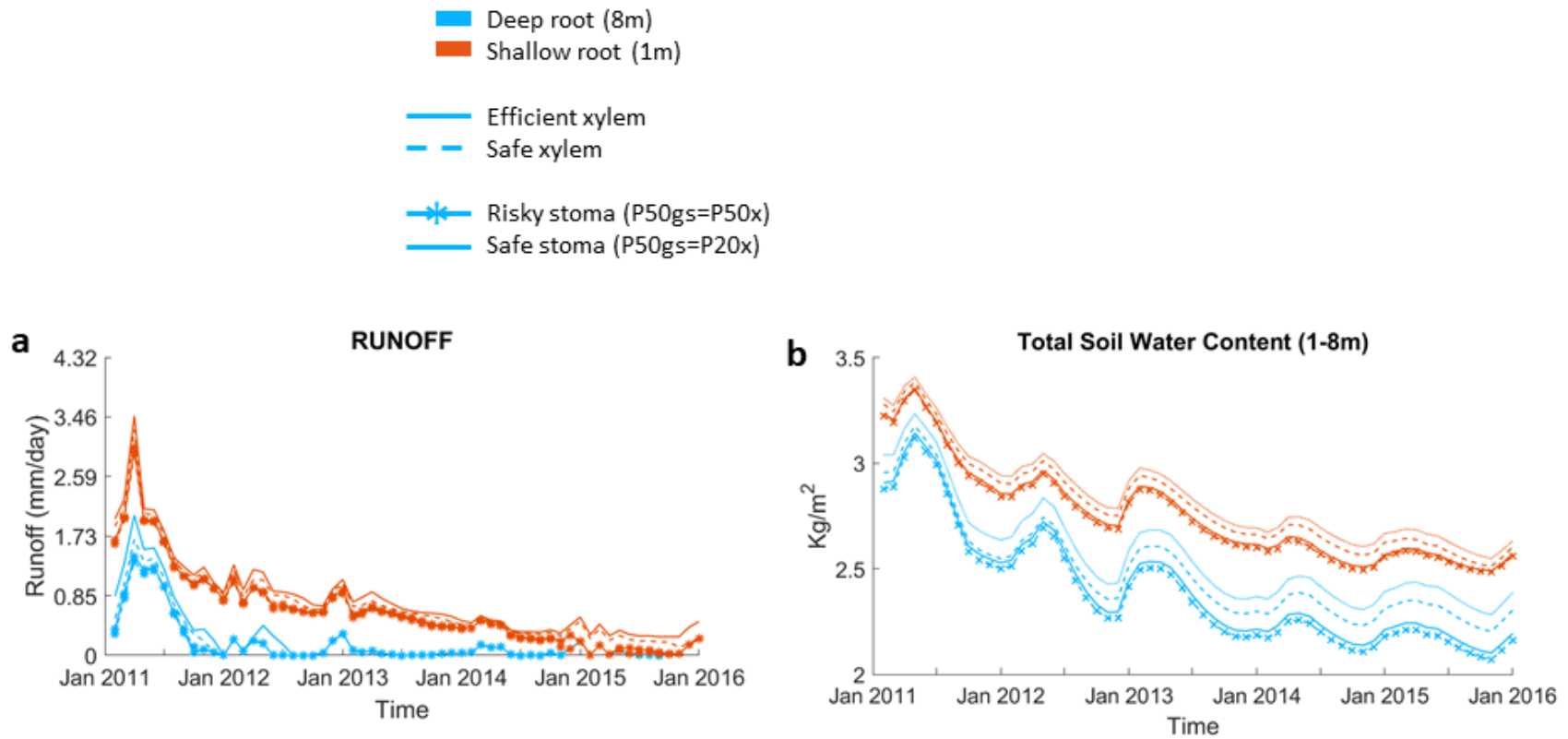
Figure 6. Impact on hydrologic processes: a) mean monthly total runoff, and b) monthly mean total soil water content of the entire soil column.
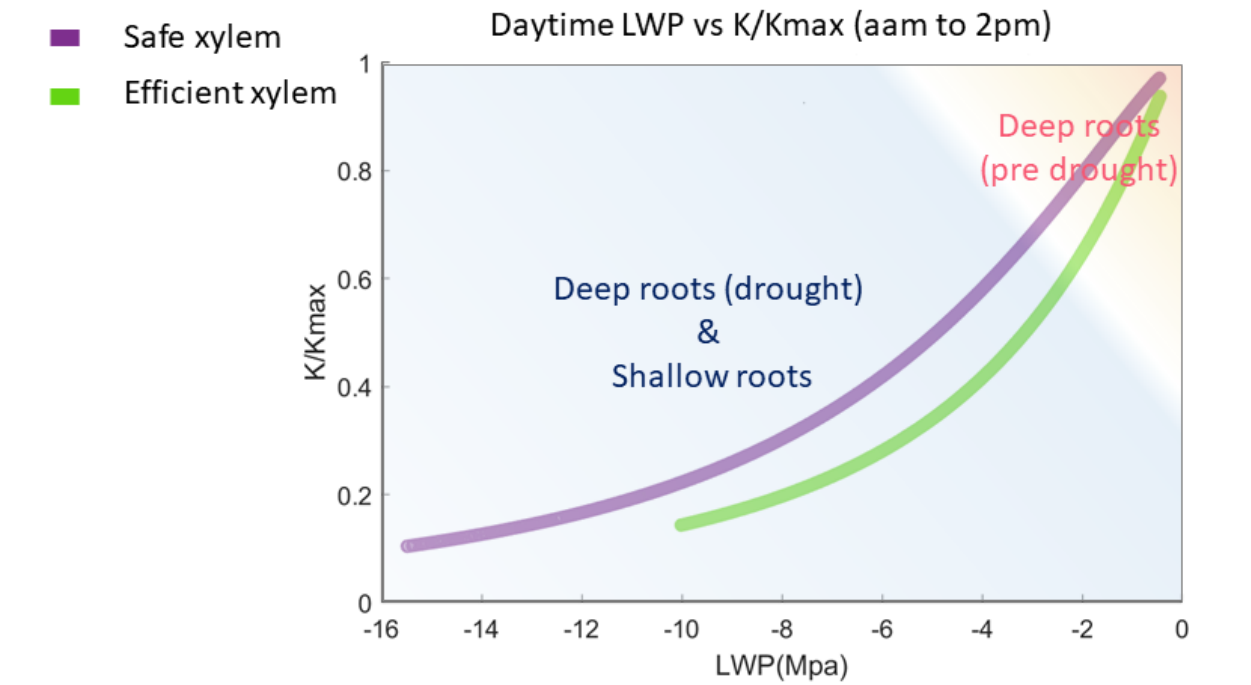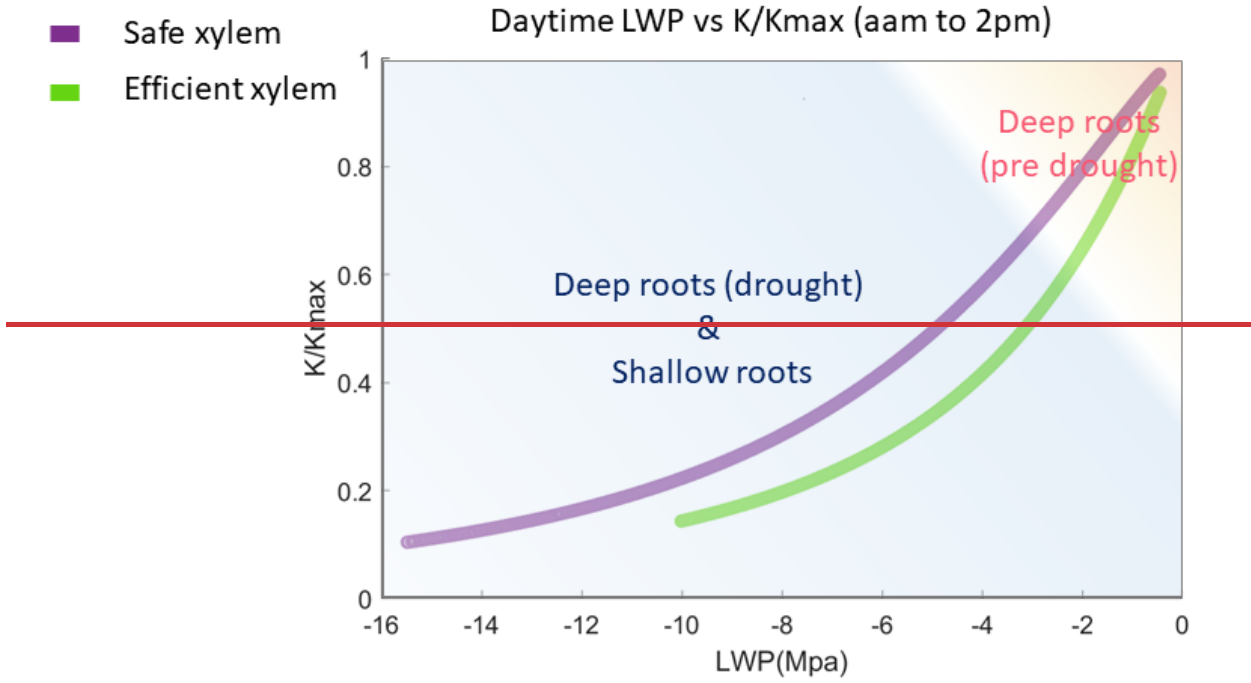
Figure 7. Simulated leaf water potential and fraction loss of conductivity (K/Kmax) of all the cases, which follow the two vulnerability curves.

Figure 8
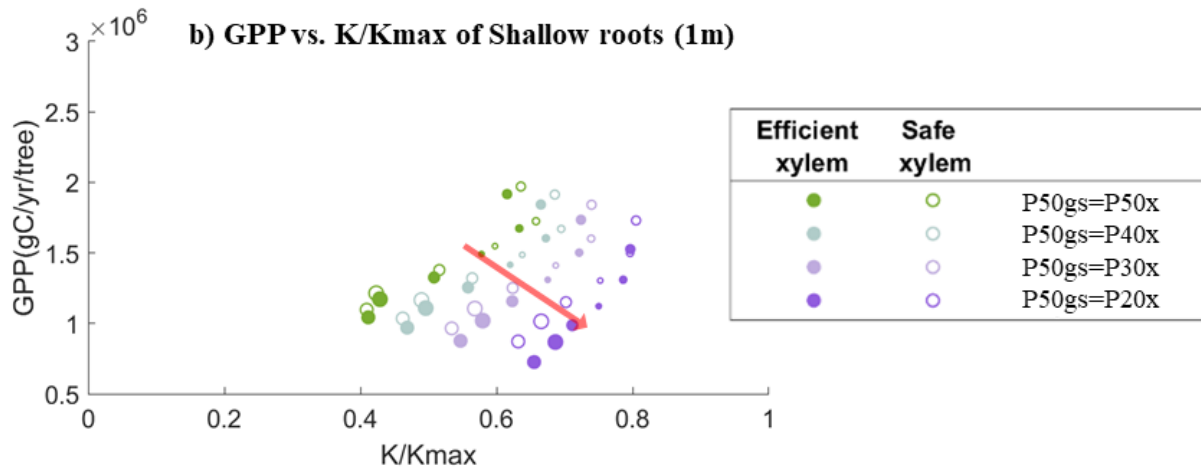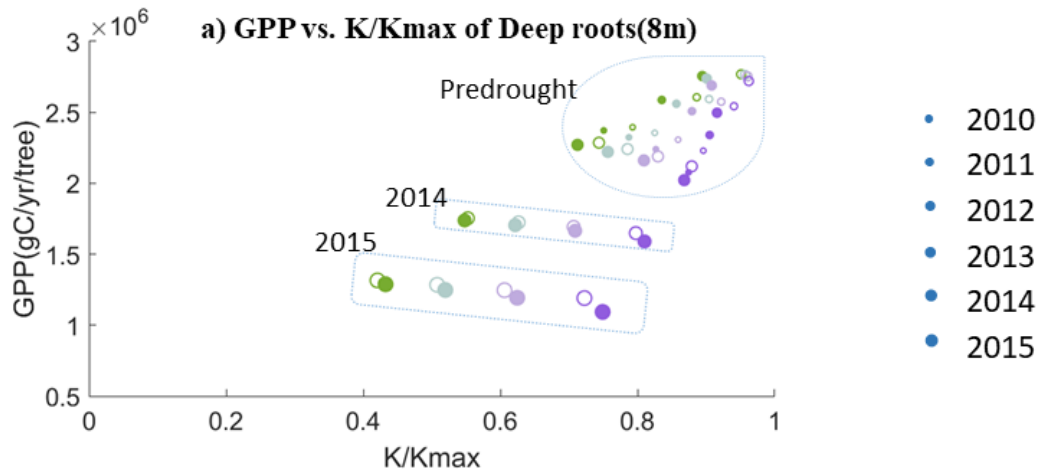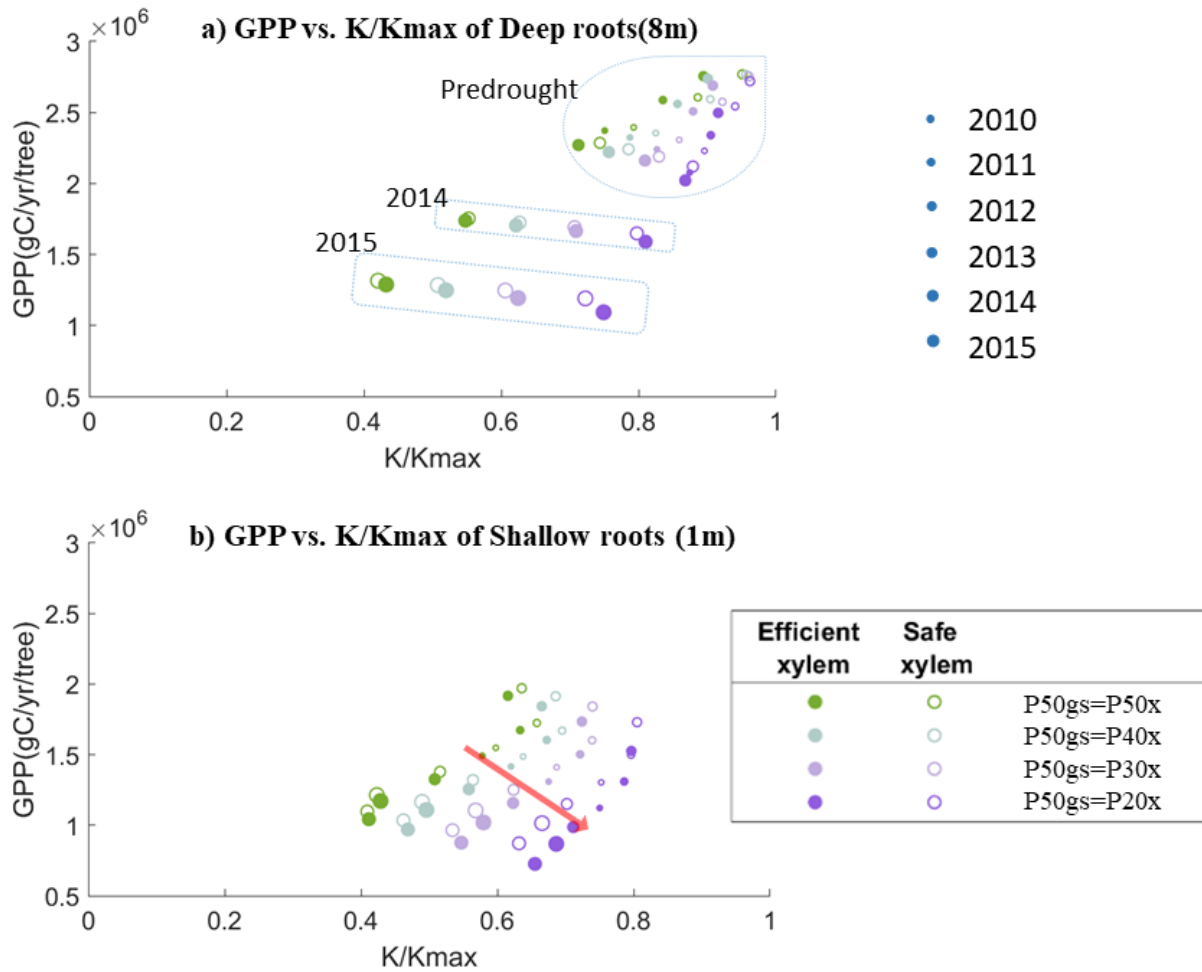
Figure 8. Simulated average annual GPP and fraction of conductance of a 55cm DBH cohort with a) deep roots (effective rooting depth= 8m) and b) shallow roots (effective rooting depth= 1m).